Progress of Theoretical Physics, Vol. 41, No. 6, June 1969

Gross Theory of Nuclear β-Decay

Kohji TAKAHASHI and Masami YAMADA*

Department of Applied Physics, Waseda University
Shinjuku-ku, Tokyo
**Science and Engineering Research Laboratory, Waseda University*
Shinjuku-ku, Tokyo

(Received January 29, 1969)

A theory for the gross properties of the nuclear β-decay is developed. In order to treat the gross features, summations over final states are replaced by integrations, and the average of the squared absolute value of the nuclear matrix element times the final level density (this quantity is denoted by $|M_\varrho(E)|^2$ where $-E$ is the decay energy) is investigated instead of individual matrix elements. First, the general slowness of the allowed β-decay is qualitatively demonstrated by the use of sum rules. Next, a model is set up in order to make quantitative calculations. In this model, an existence of "single-nucleon energies ε" is assumed, and each nucleon is assumed to make a "transition" with probability $D_\varrho(E, \varepsilon)$ as a result of the operation of the single-particle β-decay operator. $|M_\varrho(E)|^2$ is given as an integral with respect to ε, whose integrand is the product of $D_\varrho(E, \varepsilon)$ and the distribution function of nucleons over ε. Some interference effects are neglected, and the exclusion principle is introduced not in the integrand but in the lower limit of the integration domain. The half-lives of allowed β-decays are calculated with this model. At first, the Fermi gas model is used to evaluate the energy distribution of the single-nucleons. With some trial forms of $D_\varrho(E, \varepsilon)$, a reasonable agreement with experiment is obtained for odd-mass nuclei, especially for nuclei with high Q-values. Secondly, the even-odd mass difference is taken into account in a simplified way to refine the treatment of even-mass nuclei. The results show that the majority of allowed β-decays can be explained to a considerable degree by the gross theory which is utterly different from current theories of β-decay.

§ 1. Introduction

Recent theoretical study of the nuclear β-decay has been directed to two problems. One is the nature of the β-decay interaction, or more generally, of the weak interaction, and the other is the calculation of the nuclear matrix elements, though these two cannot be strictly distinguished.

The historic discovery of parity non-conservation in the β-decay in 1957 was followed by a rapid progress of our understanding of the fundamental interaction. Nevertheless, the calculation of nuclear matrix elements has been difficult except for some special cases because of the lack of our knowledge about the nuclear wave functions. For example, it is well known that the single-particle shell model gives ft-values of allowed transitions generally smaller than the observed ones by factors of ≈ 10 to ≈ 10000.[1] Although some of these hindered transitions are explained as l-forbidden ones, the majority of the matrix elements

cannot be explained even with some wave functions which seem reasonable in explaining other nuclear phenomena. For example, a recent report shows that the observed β-decay rates in the deformed region are about 20 times (8 times) lower than the values predicted by the Nilsson model (Nilsson + pairing model).[2]

The configuration mixing has been applied to these unfavored transitions and has succeeded in explaining the hindrance phenomena after large cancellation.[3] However, the numerical results are not conclusive because they are quite sensitive to the assumed strength of the residual interaction. There are other more elaborate methods which seem hopeful.[4] It remains open to question how successful they are.

Since 1961, many isobaric analog states have been discovered.[5),6] Thus, the isospin could be an approximately good quantum number even in heavier nuclei contrary to the previous belief.[7] If the isospin is conserved, and as far as the conserved vector current (CVC)[8] is assumed, the Fermi matrix element is exhausted by the analog state to which the β-transition cannot occur energetically for heavier nuclei. The actual Fermi transition can occur only as a result of isospin impurity.[9] Furthermore, the "persistent" supermultiplet may be valid for the Gamow-Teller transition.[10] From these points of view, Fujita, Ikeda and Futami have succeeded in reproducing the hindrance factors for some transitions in the spherical[11] and later in the deformed[12] regions using the commutator method.[13]

Independently, one of the present authors tried to supplement the usual (microscopic) treatment by the gross theory and explained the general slowness of allowed transitions qualitatively.[14] This theory is, in some respect, similar to as well as complementary to the theory of Fujita et al.

The gross theory is a method appropriate for dealing with certain average properties of nuclear decay processes. Although the basic concept of the gross theory will be applicable to any kind of β-decay and even to other kinds of nuclear decays, we formulate and develop it quantitatively for the allowed β-decay in this paper.

The β-decay can proceed, in general, to several energy levels of the daughter nucleus. By the gross theory, the decay properties averaged over many transitions to different final states are treated rather than properties of individual transitions to definite final states. Then, the most important and easily manageable quantity is the total decay rate which is the main object of this paper.

In § 2 gross properties of the allowed β-decay inferred from sum rules are examined qualitatively. In § 3 a model appropriate for the gross theory is introduced. The numerical results are given for odd-mass nuclei in § 4 and for nuclei including even-mass ones in consideration of the even-odd mass difference in § 5. The last section is devoted to the discussion of the results and some relating problems. In Appendix A, the gross theory for the Fermi transition is formulated in terms of the second quantization. Approximate formulas of the

integrated Fermi function (f-function) used for the electronic computing machine are given in Appendix B.

§ 2. Gross properties of allowed β-decay inferred from sum rules

The total decay constant of the allowed β-decay in the usual approximation is written as[15]

$$\lambda=\frac{m_e^5c^4}{2\pi^3\hbar^7}\sum_j\left\{|G_{\mathrm{F}}|^2\left|\int 1_j\right|^2+|G_{\mathrm{GT}}|^2\left|\int\boldsymbol{\sigma}_j\right|^2\right\}f(E_{\mathrm{I}}-E_j), \tag{1}$$

where m_e is the electron mass, G_{F} and G_{GT} are the coupling constants of the Fermi and the Gamow-Teller interactions respectively ($|G_{\mathrm{F}}|\approx1.4\times10^{-49}\,\mathrm{erg\cdot cm^3}$, $G_{\mathrm{GT}}/G_{\mathrm{F}}\approx-1.2$), and E_{I} and E_j are the energies of the initial state Ψ_{I} and the j-th final state Ψ_j respectively. (We use the masses of neutral atoms throughout this paper because the β-decay Q-value is usually defined as the difference between the atomic masses of the parent and daughter nuclides.) $\int 1_j$ and $\int\boldsymbol{\sigma}_j$ are respectively the Fermi and the Gamow-Teller matrix elements to the j-th final state ($|\int\boldsymbol{\sigma}_j|^2$ stands for $(\int\boldsymbol{\sigma}_j)^*\cdot(\int\boldsymbol{\sigma}_j)$ summed over all possible magnetic substates of the final state and averaged over initial substates), and $f(E_{\mathrm{I}}-E_j)$ is the usual integrated Fermi function (the dimensionless f-function).

In order to transfer to the gross theory, we assume that the final level density is large enough to replace the summation over j in Eq. (1) by an integration as

$$\lambda\approx\frac{m_e^5c^4}{2\pi^3\hbar^7}\int_{-Q}^{0}\{|G_{\mathrm{F}}|^2|M_{\mathrm{F}}(E)|^2+|G_{\mathrm{GT}}|^2|\boldsymbol{M}_{\mathrm{GT}}(E)|^2\}f(-E)\,dE, \tag{2}$$

where the continuous variable E corresponds to (E_j-E_{I}) in Eq. (1), and Q is the ground-state Q-value. $|M_{\mathrm{F}}(E)|^2$ and $|\boldsymbol{M}_{\mathrm{GT}}(E)|^2$ are the final level density times the squares of the matrix elements averaged in an appropriate energy interval for the Fermi and the Gamow-Teller transitions, respectively. Many decay properties which do not depend on the detailed structure of the individual final levels can be derived from these two functions $|M_{\mathrm{F}}(E)|^2$ and $|\boldsymbol{M}_{\mathrm{GT}}(E)|^2$. The replacement of discrete sums by integrations such as of Eq. (1) by Eq. (2) is essential to the gross theory and might be called the "gross approximation" or "gross treatment".

In the following general argument, we write $|M_{\mathcal{Q}}(E)|^2$ for $|M_{\mathrm{F}}(E)|^2$ or $|M_{\mathrm{GT}}^{(i)}(E)|^2$ where the superscript i indicates the part of $|\boldsymbol{M}_{\mathrm{GT}}(E)|^2$ coming from the i-th component of the vector operator $\boldsymbol{\sigma}$ ($|\boldsymbol{M}_{\mathrm{GT}}(E)|^2=\sum_i|M_{\mathrm{GT}}^{(i)}(E)|^2$). In order to see the general features of $|M_{\mathcal{Q}}(E)|^2$, it is convenient to investigate the state

$$\Phi_{\mathcal{Q}}\equiv\mathcal{Q}\Psi_{\mathrm{I}}, \tag{3}$$

where $\mathcal{Q}$ is the β-decay operator,

The unnormalized Φ_Ω-state can be characterized fairly well by the following three quantities: the square of the norm $\langle\Phi_\Omega|\Phi_\Omega\rangle$, the energy expectation value $\langle\Phi_\Omega|H|\Phi_\Omega\rangle/\langle\Phi_\Omega|\Phi_\Omega\rangle$, and the second moment of its energy distribution. These three quantities can be related with $|M_\Omega(E)|^2$ as

$$\langle\Phi_\Omega|\Phi_\Omega\rangle=\langle\Psi_{\rm I}|\Omega^\dagger\Omega|\Psi_{\rm I}\rangle=\sum_j\langle\Psi_{\rm I}|\Omega^\dagger|\Psi_j\rangle\langle\Psi_j|\Omega|\Psi_{\rm I}\rangle$$

$$=\sum_j|\langle\Psi_j|\Omega|\Psi_{\rm I}\rangle|^2\approx\int_{-Q}^{\infty}|M_\Omega(E)|^2dE\,, \tag{4}$$

$$\frac{\langle\Phi_\Omega|(H-E_{\rm I})|\Phi_\Omega\rangle}{\langle\Phi_\Omega|\Phi_\Omega\rangle}=\frac{\langle\Psi_{\rm I}|\Omega^\dagger[H,\Omega]|\Psi_{\rm I}\rangle}{\langle\Psi_{\rm I}|\Omega^\dagger\Omega|\Psi_{\rm I}\rangle}=\frac{\sum_j\langle\Psi_{\rm I}|\Omega^\dagger|\Psi_j\rangle\langle\Psi_j|[H,\Omega]|\Psi_{\rm I}\rangle}{\sum_j\langle\Psi_{\rm I}|\Omega^\dagger|\Psi_j\rangle\langle\Psi_j|\Omega|\Psi_{\rm I}\rangle}$$

$$=\frac{\sum_j(E_j-E_{\rm I})|\langle\Psi_j|\Omega|\Psi_{\rm I}\rangle|^2}{\sum_j|\langle\Psi_j|\Omega|\Psi_{\rm I}\rangle|^2}\approx\frac{\int_{-Q}^{\infty}E|M_\Omega(E)|^2dE}{\int_{-Q}^{\infty}|M_\Omega(E)|^2dE}\,, \tag{5}$$

$$M_2=\frac{\langle\Phi_\Omega|(H-E_{\rm I})^2|\Phi_\Omega\rangle}{\langle\Phi_\Omega|\Phi_\Omega\rangle}=\frac{\langle\Psi_{\rm I}|[\Omega^\dagger,H][H,\Omega]|\Psi_{\rm I}\rangle}{\langle\Psi_{\rm I}|\Omega^\dagger\Omega|\Psi_{\rm I}\rangle}$$

$$=\frac{\sum_j\langle\Psi_{\rm I}|[\Omega^\dagger,H]|\Psi_j\rangle\langle\Psi_j|[H,\Omega]|\Psi_{\rm I}\rangle}{\sum_j\langle\Psi_{\rm I}|\Omega^\dagger|\Psi_j\rangle\langle\Psi_j|\Omega|\Psi_{\rm I}\rangle}$$

$$=\frac{\sum_j(E_j-E_{\rm I})^2|\langle\Psi_j|\Omega|\Psi_{\rm I}\rangle|^2}{\sum_j|\langle\Psi_j|\Omega|\Psi_{\rm I}\rangle|^2}\approx\frac{\int_{-Q}^{\infty}E^2|M_\Omega(E)|^2dE}{\int_{-Q}^{\infty}|M_\Omega(E)|^2dE}\,, \tag{6}$$

where uses are made of the sum rules and the gross approximation. Equations (4) $\sim$ (6) reduce the problem of the requisite distribution function $|M_\Omega(E)|^2$ to that of the Φ_Ω-state.

The β-decay operator can be written as $\Omega=\sum_k\omega_k$ with the single-particle operator ω_k which operates on the k-th nucleon. For the $\beta^\pm$ Fermi transition, $\omega_k=\tau_k^{\mp}=\frac{1}{2}(\tau_k^{(1)}\mp i\tau_k^{(2)})$ ($\tau^{(3)}=+1$ for proton and -1 for neutron), and for the Gamow-Teller transition, $\omega_k=\tau_k^{\mp}\sigma_k^{(i)}$. In this notation, the left side of Eq. (4) is

$$\langle\Phi_\Omega|\Phi_\Omega\rangle=\sum_k\langle\Psi_{\rm I}|\omega_k^\dagger\omega_k|\Psi_{\rm I}\rangle+\sum_{l>m}\langle\Psi_{\rm I}|\omega_l^\dagger\omega_m+\omega_m^\dagger\omega_l|\Psi_{\rm I}\rangle\,. \tag{7}$$

This equation gives

$$\langle\Phi_\Omega|\Phi_\Omega\rangle_{\rm F}=N_1+(P_3-P_1)NZ \tag{8}$$

for the Fermi transition, where N_1 is the total number of nucleons having a possibility of decay, i.e. the total proton number Z for β^+-decay and the total neutron number N for β^--decay. P_3 and P_1 are the probabilities of finding a neutron-proton pair in isospin triplet and singlet states, respectively. If the parent nucleus is unpolarized, Eq. (7) gives

$$\langle\Phi_\Omega|\Phi_\Omega\rangle_{\rm GT}=N_1+(\tfrac{1}{3}P_{33}+P_{11}-\tfrac{1}{3}P_{13}-P_{31})NZ \tag{9}$$

for the Gamow-Teller transition, where P_{33}, P_{11}, P_{13} and P_{31} are the probabilities of finding a neutron-proton pair in isospin triplet and spin triplet, isospin singlet

and spin singlet, isospin singlet and spin triplet, and isospin triplet and spin singlet states, respectively. In the usual models (e.g. the shell model), the right sides of Eqs. (8) and (9) are considerably smaller than N_1.

The nuclear Hamiltonian H may be written in the non-relativistic approximation as

$$H \approx H_K + H_N + H_C , \tag{10}$$

where H_K is the kinetic energy, H_N the nuclear force potential and H_C the sum of the Coulomb energy and the neutron-hydrogen mass difference. In order to estimate (5) and (6), the commutation relation between the Hamiltonian (10) and the β-decay operator is necessary. In the case of the allowed β-decay the operator commutes with H_K if the small effect due to the neutron-proton mass difference is neglected. Furthermore, the charge independence of nuclear forces leads to

$$[H_N, T_\mp] = 0 \tag{11}$$

for the $\beta^\pm$ Fermi transition with $T_\mp = T^{(1)} \mp iT^{(2)} = \sum_k \tau_k^\mp$. Although a possible charge-dependent part of nuclear forces is hard to separate, it is probably very small.[16] Therefore, we consider only the Coulomb term as a charge-dependent one:

$$H_C = \frac{1}{2} \sum_{k \neq l} \frac{1+\tau_k^{(3)}}{2} \frac{1+\tau_l^{(3)}}{2} \frac{e^2}{r_{kl}} + \Delta_{nH} \sum_m \frac{1-\tau_m^{(3)}}{2} , \tag{12}$$

where Δ_{nH} is the neutron-hydrogen mass difference. With Eqs. (11) and (12) the first equation in (5) can be explicitly written as

$$\begin{aligned} \frac{\langle \Phi_\varrho | (H-E_I) | \Phi_\varrho \rangle_F}{\langle \Phi_\varrho | \Phi_\varrho \rangle_F} &\approx \frac{\langle \Psi_I | T_\pm [H_C, T_\mp] | \Psi_I \rangle}{\langle \Psi_I | T_\pm T_\mp | \Psi_I \rangle} \\ &= \mp \left\{ \frac{\langle \Phi_\varrho | \sum_{k \neq l} ((1+\tau_l^{(3)})/2)\, (e^2/r_{kl})\, \tau_k^\mp | \Psi_I \rangle}{\langle \Phi_\varrho | \Phi_\varrho \rangle} - \Delta_{nH} \right\} \end{aligned} \tag{13}$$

for $\beta^\pm$-decay. This equation indicates that the energy expectation value of the Φ_ϱ-state is smaller than the initial energy E_I for β^+-decay and is larger for β^--decay; these energy differences equal to the Coulomb energy of the decaying nucleon minus Δ_{nH}. According to Eq. (5), the average energy of the distribution function $|M_F(E)|^2$ is determined from this energy difference.

As far as the Coulomb force is concerned, the same effect is expected in the case of the Gamow-Teller transition. However, the spin-dependent part of nuclear forces H_N (e.g. the Bartlett and Heisenberg exchange forces, the tensor force, the spin-orbit force) does not commute with the Gamow-Teller operator. It is possible to estimate the commutator with a certain form of nuclear potential.[11] However, such an estimate is not conclusive quantitatively because of the lack of our knowledge about the accurate form of nuclear forces, so that we do not give explicit expressions. It is inferred that the spin-dependent part of

nuclear forces somewhat increases the average energy of $|M_{GT}^{(i)}(E)|^2$, because the Gamow-Teller operator disturbs the orientations of the nucleon spins which are arranged to minimize the energy in the initial ground state. The energy increase, however, is probably not very large since the orientations of the initial nucleon spins are not expected to be much different from random ones. Thus, the energy center of $|M_{GT}^{(i)}(E)|^2$ will be situated not so far from that of $|M_F(E)|^2$.

It should be noted that the Φ_ϱ-state is not an energy eigenstate. The Coulomb energy, for example, is different from the average one depending on the position of the decaying nucleon. At the center of the nucleus or near another proton the Coulomb energy is larger than the average, while at the periphery it is smaller. These effects are the causes of the energy spread of $|M_F(E)|^2$, which is very small as observed on the isobaric analog states. On the other hand, the effect of spin flip in the Gamow-Teller transition will make the energy spread of $|M_{GT}^{(i)}(E)|^2$ much larger than that of $|M_F(E)|^2$.

Except for some special cases in light nuclei, the transition can occur only to the "tail" part of the distribution function $|M_\varrho(E)|^2$, because the greater part of the function is situated far from the energetically reachable region. According as the energy spread becomes wider, the area of the tail part, in which the energetically reachable region falls, becomes larger. Thus, it can be easily understood that the Fermi transition with the narrower energy spread is generally more hindered than the Gamow-Teller transition and even the latter is much slower than the single-particle estimate. The superallowed transition can be explained as such a case that the peak of the distribution function $|M_\varrho(E)|^2$ exists in the energetically reachable region $0 \geqq E \geqq -Q$.

§ 3. A model for gross theory

In this section, a model appropriate to the gross theory is set up and the argument of § 2 is developed quantitatively. Since the β-decay operator is a sum of single-particle operators, the energy difference E can be regarded, in a sense, as the difference between the energies of the decaying single nucleon in the daughter and parent nuclei. Here we assume the existence of such "single-nucleon energies" and denote this energy in the parent nucleus by ε. The shell model is the simplest picture of this kind, but our picture might have a wider range of applicability.

The single-nucleon energy ε can be defined as a sum of the kinetic energy, the potential energy between that nucleon and the others, and the energy of the neutron-proton mass difference. When the nucleon under consideration is not very close to the other nucleons, ε will be of the order of the energy of the shell-model particle. However, when the nucleon lies close to another nucleon, a strong attractive force between them may reduce that energy. The repulsive part of the nuclear potential seems to be not so effective as the attractive one, because the nucleons in the ground state of the parent nucleus tend to avoid

the repulsive potential to minimize the total energy. Thus, the distribution of the single-nucleon energies is something like that of the energies of nucleons contained in a vessel. The bottom of the vessel changes with time, or more strictly, is a superposition of many kinds of uneven shapes. The effect coming from this uncertainty of the bottom shape is small in the β-decay as is discussed in § 4. This vessel and the single-nucleon states of the parent nucleus are schematically illustrated in Fig. 1 for β^--decay by assuming flat Fermi surfaces. Actually, the surfaces may be diffused by the nucleon-nucleon interaction. The nucleon number N_1 introduced in Eqs. (8) and (9) can be written as an integral,

$$N_1 = \int_{\varepsilon_{\min}}^{\varepsilon_1} \frac{dN_1}{d\varepsilon} d\varepsilon \,, \tag{14}$$

where $\varepsilon_{\min}$ is the single-nucleon energy at the bottom of the vessel, ε_1 is the maximum energy of the filled single-nucleon states, and $dN_1/d\varepsilon$ is the number density of nucleon having a possibility of decay.

When the nucleon with energy ε transforms from a neutron into a proton or from a proton into a neutron as a result of the operation of the single β-decay operator ω_k, the energy of the nucleus is changed. At first, we neglect the Pauli exclusion principle during this transition, and denote the probability that the energy increase equals to $(E_j - E_1)$ by $P_\varrho(E_j - E_1, \varepsilon)$. Then, the equation

$$\sum_j P_\varrho(E_j - E_1, \varepsilon) = 1 \tag{15}$$

holds for the allowed decay, because the operator ω_k necessarily changes the sign of the third component of the isospin of the k-th nucleon leaving the amplitude unchanged as a whole. The probability distribution function $D_\varrho(E, \varepsilon)$ is defined in the gross approximation as the product of the energy average of P_ϱ and the final level density. By Eq. (15),

$$\int_{-\infty}^{\infty} D_\varrho(E, \varepsilon)\, dE \approx \sum_j P_\varrho(E_j - E_1, \varepsilon) = 1 \,. \tag{16}$$

Up to this stage of argument, every nucleon has been urged to have a unit potentiality of decay in disregard of the possibility that the transition might be inhibited by energetics or by the Pauli principle. In this point, our treatment is utterly different from the usual microscopic models.

The distribution function $|M_\varrho(E)|^2$ will be written as an integral of the product of $D_\varrho(E, \varepsilon)$

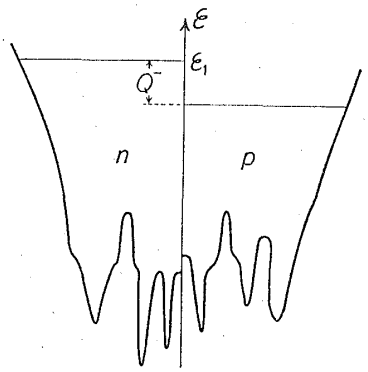

Fig. 1. Schematic illustration of the single-nucleon states in the flat-surface approximation for β^--decay. ε: single-nucleon energy. ε_1: maximum energy of the filled single-nucleon states. Q^-: ground-state Q-value. For β^+-decay and electron capture the roles of neutrons and protons are interchanged and Q^- is replaced by Q_ε.

and $dN_1/d\varepsilon$. We assume that the effect of the Pauli principle can be included in the lower limit of the integration domain as follows:

$$|M_\Omega(E)|^2 \approx \int_{\varepsilon_0(E)}^{\varepsilon_1} D_\Omega(E,\varepsilon)\frac{dN_1}{d\varepsilon}d\varepsilon\,. \tag{17}$$

For example, in the case of the flat surface (Fig. 1), the Pauli principle can be expressed by an inequality as

$$\varepsilon + E > \varepsilon_1 - Q\,, \tag{18}$$

and the lower limit of the integration domain of (17) is written as

$$\varepsilon_0(E) = \max(\varepsilon_{\min}, \varepsilon_1 - Q - E)\,, \tag{19}$$

where $\max(a, b)$ denotes the larger one of a and b.

Equation (17) represents our model appropriate to the gross theory. It has a rather general form and the forms of $D_\Omega(E,\varepsilon)$, $dN_1/d\varepsilon$ and $\varepsilon_0(E)$ are still left unspecified. Equation (17) has two characteristic features. The first is the neglect of the quantum-mechanical interference effect coming from the fact that the β-decay operator is not a mere single-particle operator but a sum of single-particle operators. In other words, the coherent character of the decay is not considered at all. Secondly, the Pauli principle is introduced not in the integrand but in the lower limit of the integration domain.

The understanding of the approximaton leading to Eq. (17) may be helped by the following expressions for the Φ_Ω-state:

$$\Phi_\Omega \approx \sum_j \sum_{\substack{\varepsilon \\ \{\text{incoh}\} \\ \{\text{Pauli}\}}} \sqrt{P_\Omega(E_j - E_1, \varepsilon)}\,\Psi_j(E_j)\,, \tag{20}$$

or with D_Ω,

$$\Phi_\Omega \approx \int \sum_{\substack{\varepsilon \\ \{\text{incoh}\} \\ \{\text{Pauli}\}}} \sqrt{D_\Omega(E,\varepsilon)}\,\Psi(E_1 + E)\,dE\,, \tag{21}$$

where the summation over ε is taken incoherently and the Pauli principle is considered in the method of summation.

When the surface diffuseness is worth due consideration, the expression (17) may be replaced by

$$|M_\Omega(E)|^2 \approx \int_{\varepsilon_0(E)}^{\varepsilon_1} D_\Omega(E,\varepsilon)\frac{dN_1}{d\varepsilon}W(E,\varepsilon)\,d\varepsilon\,, \tag{22}$$

with

$$0 \leqq W(E,\varepsilon) \leqq 1\,. \tag{23}$$

Here, $W(E,\varepsilon)$ is a weight function which reflects the availability (the degree of vacancy) of the final states. In the special case of the flat surface, $W(E,\varepsilon)$

equals to unity for $\varepsilon+E>\varepsilon_1-Q$ and vanishes for $\varepsilon+E\leqq\varepsilon_1-Q$, so that the difference between Eqs. (17) and (22) disappears.

In the case of the flat surface, the total decay rate (2) can be written with Eqs. (17) and (19) as

$$\lambda=\frac{m_e{}^5c^4}{2\pi^3\hbar^7}\int_{-Q}^{0}\int_{\max(\varepsilon_{\min},\,\varepsilon_1-Q-E)}^{\varepsilon_1}\{|G_{\mathrm{F}}|^2D_{\mathrm{F}}(E,\varepsilon)+3|G_{\mathrm{GT}}|^2D_{\mathrm{GT}}(E,\varepsilon)\}\frac{dN_1}{d\varepsilon}f(-E)\,d\varepsilon dE\,, \quad (24)$$

where the coefficient 3 of the Gamow-Teller term comes from the assumption that the parent nucleus is unpolarized. In the case of the diffuse surface, it can be written with Eq. (22) as

$$\lambda=\frac{m_e{}^5c^4}{2\pi^3\hbar^7}\int_{-Q}^{0}\int_{\varepsilon_0(E)}^{\varepsilon_1}\{|G_{\mathrm{F}}|^2D_{\mathrm{F}}(E,\varepsilon)+3|G_{\mathrm{GT}}|^2D_{\mathrm{GT}}(E,\varepsilon)\}\frac{dN_1}{d\varepsilon}W(E,\varepsilon)f(-E)\,d\varepsilon dE\,. \quad (25)$$

The approximation leading to our model is further investigated in terms of

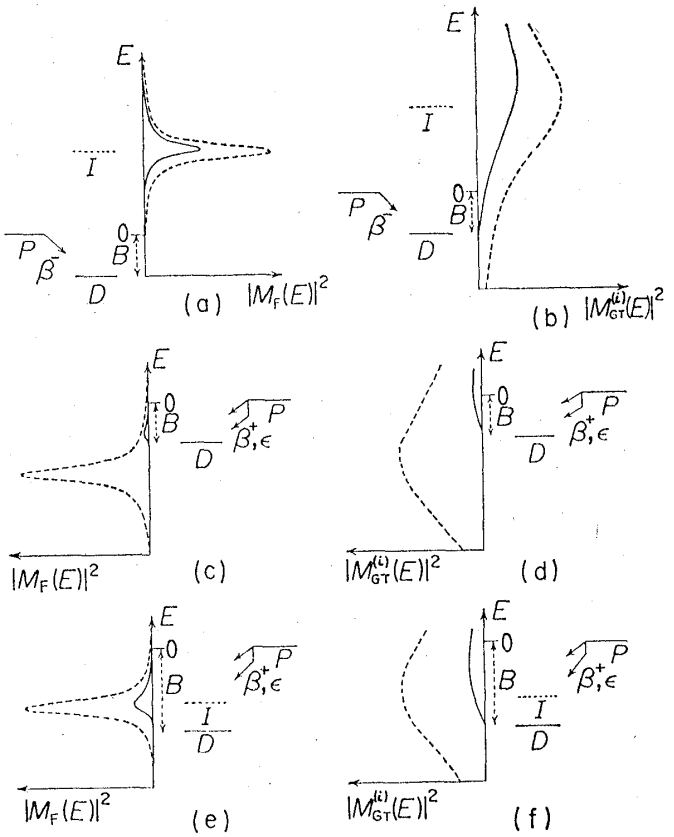

Fig. 2. Schematic illustration of our model for the gross theory. The solid lines represent $|M_{\mathrm{F}}(E)|^2$ ((a), (c), (e)) and $|M_{\mathrm{GT}}{}^{(i)}(E)|^2$ ((b), (d), (f)), and dashed lines correspond to the cases in which the Pauli principle is neglected by putting $\varepsilon_0(E)\to\varepsilon_{\min}$. Figures (e) and (f) correspond to the superallowed transition. P: parent nucleus, D: daughter nucleus, I: isobaric analog state, B: the range to which actual β-decay proceeds.

the second quantization in Appendix A. There, it will be shown that $D_\varrho(E, \varepsilon)$ has properties qualitatively similar to those of $|M_\varrho(E)|^2$ discussed in § 2; i.e. the energy center of $D_F(E, \varepsilon)$ as a function of E is situated very close to the isobaric analog state and the energy spread is very small, and for the Gamow-Teller transition the spin-dependent part of nuclear forces makes the spread of $D_{GT}(E, \varepsilon)$ much wider. Figure 2 illustrates our model schematically.

§ 4. Calculations with the Fermi gas model

The Fermi gas model is the simplest model adequate to the estimate of $dN_1/d\varepsilon$ and $\varepsilon_0(E)$ in Eq. (17). In this model,

$$\frac{dN_1}{d\varepsilon}=\frac{2}{(2\pi\hbar)^3}4\pi V[2M_n^{*3}(\varepsilon-\varepsilon_{min})]^{1/2}, \tag{26}$$

$$\varepsilon_{min}=\varepsilon_1-\varepsilon_F\,. \tag{27}$$

Here, M_n^* is the effective mass of nucleon, V is the appropriate nuclear volume, and ε_F is the Fermi energy given by

$$\varepsilon_F=\frac{\hbar^2}{2M_n^*}\left(3\pi^2\frac{N_1}{V}\right)^{2/3}. \tag{28}$$

If we denote the nucleon mass by M_n and the nuclear radius by $R=r_0\cdot A^{1/3}$ fm, where A is the mass number, Eq. (28) becomes

$$\varepsilon_F=\frac{76.52}{(M_n^*/M_n)r_0^2}\left(\frac{N_1}{A}\right)^{2/3}\ \text{MeV}. \tag{29}$$

We take $r_0=1.2$ and

$$M_n^*/M_n=0.6\ ^{17)} \tag{30}$$

in the following numerical calculations.

In actual cases, Eq. (19) can be replaced by

$$\varepsilon_0(E)=\varepsilon_1-Q-E\,, \tag{31}$$

and the single nucleons with energy $\varepsilon<\varepsilon_1-Q$ do not participate in the actual β-decay. Therefore, the bottom shape of the vessel in Fig. 1 has little influence on the β-decay.

Next, the distribution function $D_\varrho(E, \varepsilon)$ must be determined. For simplicity, we neglect its ε-dependence; i.e. we assume that every nucleon has the same decay potentiality no matter what the energy ε of the nucleon is. Then, with Eqs. (26), (27), (28) and (31) the integration of Eq. (17) can be carried out and Eq. (24) becomes

$$\lambda=\frac{m_e^5c^4}{2\pi^3\hbar^7}\int_{-Q}^{0}\{|G_F|^2D_F(E)+3|G_{GT}|^2D_{GT}(E)\}N_1\left[1-\left(1-\frac{Q+E}{\varepsilon_F}\right)^{3/2}\right]f(-E)\,dE\,. \tag{32}$$

For the function $f(-E)$ we use the approximate expression given in Appendix B. The quantity in the square brackets in Eq. (32) represents the effect of the Pauli principle.

Although we have some qualitative information about $D_{\mathrm{F}}(E)$ and $D_{\mathrm{GT}}(E)$ as mentioned at the end of § 3, there is little information about their detailed behavior. Hence, we assume some trial forms.

After Dyson,[18] we start with the Gaussian type.

1. *Gaussian type*: For the Fermi transition,

$$D_{\mathrm{F}}(E)=\frac{1}{\sqrt{2\pi}\sigma_{\mathrm{F}}}\exp\{-(E-\Delta_{\mathrm{F}})^2/(2\sigma_{\mathrm{F}}^2)\}, \tag{33}$$

where the energy center Δ_{F} and the standard deviation σ_{F} can be attributed to the Coulomb force:

$$\Delta_{\mathrm{F}}=\Delta_{\mathrm{C}}, \tag{34}$$

$$\sigma_{\mathrm{F}}=\sigma_{\mathrm{C}}, \tag{35}$$

whose explicit forms will be given later. For the Gamow-Teller transition,

$$D_{\mathrm{GT}}(E)=\frac{1}{\sqrt{2\pi}\sigma_{\mathrm{GT}}}\exp\{-(E-\Delta_{\mathrm{GT}})^2/(2\sigma_{\mathrm{GT}}^2)\}. \tag{36}$$

Here, we approximate as

$$\Delta_{\mathrm{GT}}\approx\Delta_{\mathrm{F}}=\Delta_{\mathrm{C}}, \tag{37}$$

$$\sigma_{\mathrm{GT}}^2=\sigma_{\mathrm{C}}^2+\sigma_{\mathrm{N}}^2, \tag{38}$$

where σ_{N} is the energy spread caused by the spin-dependent part of nuclear forces.

2. *Exponential type*:

$$D_{\mathrm{F}}(E)=\frac{1}{\sqrt{2}\sigma_{\mathrm{F}}}\exp\{-\sqrt{2}|E-\Delta_{\mathrm{F}}|/\sigma_{\mathrm{F}}\}, \tag{39}$$

$$D_{\mathrm{GT}}(E)=\frac{1}{\sqrt{2}\sigma_{\mathrm{GT}}}\exp\{-\sqrt{2}|E-\Delta_{\mathrm{GT}}|/\sigma_{\mathrm{GT}}\}. \tag{40}$$

These functions are not differentiable at $E=\Delta_{\mathrm{F}}$ or Δ_{GT}, but this behavior does not come into question except for light nuclei. For σ_{GT}, Eq. (38) is used. Other expressions for σ_{GT} as a function of σ_{N} and σ_{C} do not alter the result significantly because $\sigma_{\mathrm{GT}}\approx\sigma_{\mathrm{N}}\gg\sigma_{\mathrm{C}}$.

3. *Modified-Lorentz type*:

$$D_{\mathrm{F}}(E)=\frac{(\sigma_{\mathrm{F}}^2+\gamma^2)(\sigma_{\mathrm{F}}^2/\gamma)}{\pi}\frac{1}{(E-\Delta_{\mathrm{F}})^2+(\sigma_{\mathrm{F}}^2/\gamma)^2}\frac{1}{(E-\Delta_{\mathrm{F}})^2+\gamma^2}, \tag{41}$$

$$D_{\mathrm{GT}}(E)=\frac{(\sigma_{\mathrm{GT}}^2+\gamma^2)(\sigma_{\mathrm{GT}}^2/\gamma)}{\pi}\frac{1}{(E-\Delta_{\mathrm{GT}})^2+(\sigma_{\mathrm{GT}}^2/\gamma)^2}\frac{1}{(E-\Delta_{\mathrm{GT}})^2+\gamma^2}, \tag{42}$$

where γ is an adjustable parameter having the dimension of energy. If we make γ infinity keeping the quantity $\sigma_{\mathcal{Q}}^2/\gamma$ constant, the distribution function converges to the Lorentz-type function with the half-width $\Gamma_{\mathcal{Q}}/2=\sigma_{\mathcal{Q}}^2/\gamma$. Again, Eq. (38) is used for σ_{GT}.

4. *Lorentz type*:

$$D_{\mathrm{F}}(E)=\frac{\Gamma_{\mathrm{F}}}{2\pi}\frac{1}{(E-\Delta_{\mathrm{F}})^2+(\Gamma_{\mathrm{F}}/2)^2}, \tag{43}$$

$$D_{\mathrm{GT}}(E)=\frac{\Gamma_{\mathrm{GT}}}{2\pi}\frac{1}{(E-\Delta_{\mathrm{GT}})^2+(\Gamma_{\mathrm{GT}}/2)^2}. \tag{44}$$

The second moment diverges in this type of distribution function. For the Fermi transition, we assume that the (Z, A)-dependence of Γ_{F} is related to that of σ_{C} by $\Gamma_{\mathrm{F}}/2=\Gamma_{\mathrm{C}}/2=\sigma_{\mathrm{C}}^2/\gamma_0$. Here, the choice of γ_0 is rather arbitrary; we take $\gamma_0=220$ MeV. (By this choice and Eq. (46), we have $\Gamma_{\mathrm{F}}\approx 18$ keV for $Z=40$ and ≈ 40 keV for $Z=80$.) For the Gamow-Teller transition, we assume $\Gamma_{\mathrm{GT}}^2=\Gamma_{\mathrm{C}}^2+\Gamma_{\mathrm{N}}^2$ where Γ_{N} corresponds to σ_{N}.

The quantity Δ_{C} may be regarded as the single-particle Coulomb displacement. If we assume the nucleus as a uniformly charged sphere with the radius $1.2A^{1/3}$ fm, we get for $\beta^{\pm}$-decay,

$$\Delta_{\mathrm{C}}=\mp(1.44Z_1A^{-1/3}-0.7825)\ \mathrm{MeV}, \tag{45}$$

where Z_1 is the proton number of the daughter nucleus for β^+-decay and of the parent one for β^--decay.

We estimate the quantity σ_{C} as the fluctuation (or the standard deviation) of the Coulomb energy of the single decaying nucleon in the average field, assuming that the nucleon decays uniformly in the nucleus;

$$\sigma_{\mathrm{C}}=0.157Z_1A^{-1/3}\ \mathrm{MeV}. \tag{46}$$

Using the Fermi gas model, Lane and Soper estimated the fluctuation of the Coulomb energy in the whole nucleus.[7] The second moment obtained by them contains another term, which could be included in our model (cf. Appendix A, in particular, the discussion on the second term of (A23)) but is omitted in our numerical calculation.

As far as the Fermi transition is treated together with the Gamow-Teller transition, the fine structure of $D_{\mathrm{F}}(E)$ generally has little influence on the numerical results. The detailed knowledge of $D_{\mathrm{F}}(E)$ will be needed only if the Fermi transition is studied separately.

Finally, we mention the only remaining quantity σ_{N} which is the energy spread caused by the spin-dependent part of nuclear forces. Since the information on the nuclear forces is not conclusive as mentioned in § 2, we determine σ_{N} empirically. The effects of nuclear forces on a nucleon in the nucleus are fairly independent of Z and A because of the saturation property. Therefore,

we take σ_N as an adjustable parameter neglecting the (Z, A)-dependence.

A comparison of our theory with experiment is performed as follows. First, we take the experimental data on the β-decay half-lives of nuclei[19] that fulfill the following two criteria:

I. The total branching ratio of the allowed transitions exceeds or seems to exceed 50%.

II. The ground-state Q-value[19),20)] is large enough to satisfy the inequality

$$Q \geqq 10A^{-1/3} \text{ MeV} . \tag{47}$$

The first criterion is necessary because only the allowed decay is treated in this paper, and the second one is imposed to validate the assumption in our gross treatment that the final level density is large. In fact, the larger the Q-value, the better the gross approximation. In this respect, a larger lower bound of Q is preferred, but then the total number of qualified nuclei becomes too small to get statistically reliable results. The right-hand side of the inequality (47) is a compromise between these two tendencies. Figure 3 shows how the mass numbers of the nuclei fulfilling the above two criteria are distributed.

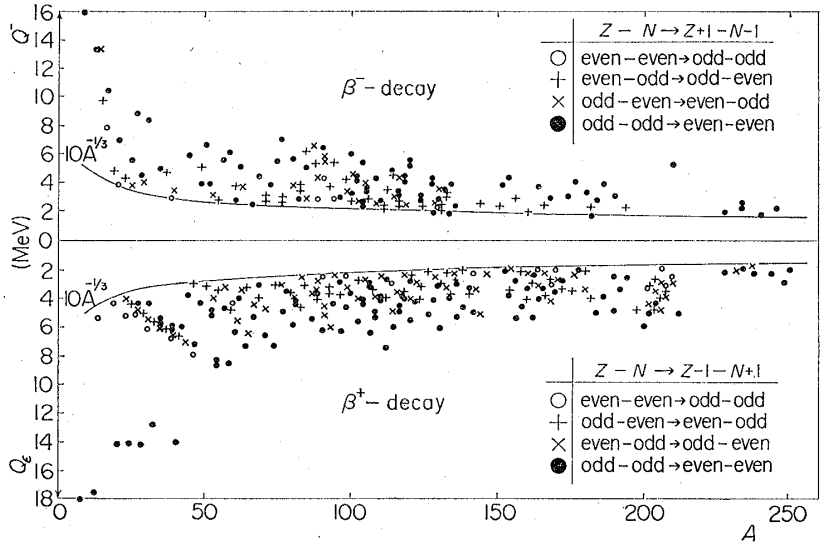

Fig. 3. The ground-state Q-values of the qualified nuclei. The second criterion (47) is shown by curves.

We determine the value of the adjustable parameter σ_N so as to minimize the quantity

$$S=\sum_{n=1}^{N_0}[\log_{10}(\tau_{1/2}^{\text{cal}}(n)/\tau_{1/2}^{\text{exp}}(n))]^2, \tag{48}$$

which is a measure of the fit between the theory and experiment. Here, the summation is taken over N_0 nuclei fulfilling the above criteria, and $\tau_{1/2}^{\text{cal}}(n)$ and $\tau_{1/2}^{\text{exp}}(n)$ are the calculated and experimental values of the β-decay half-life of the

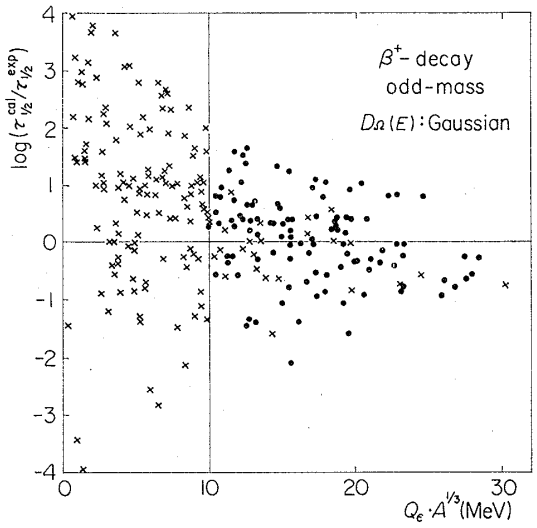

(a)

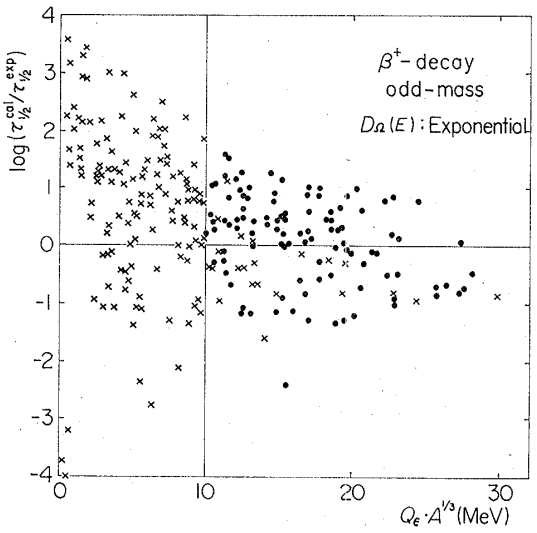

(b)

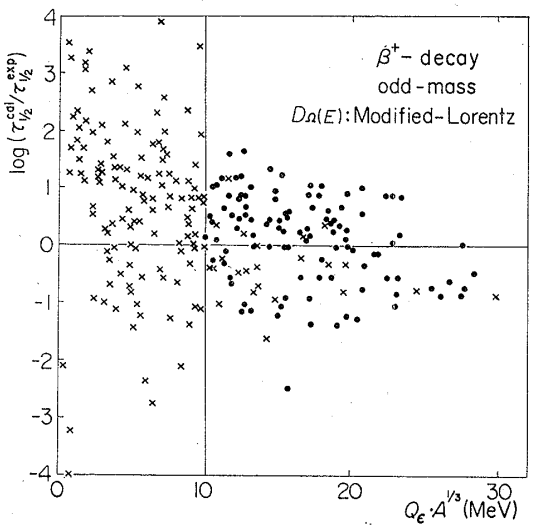

(c)

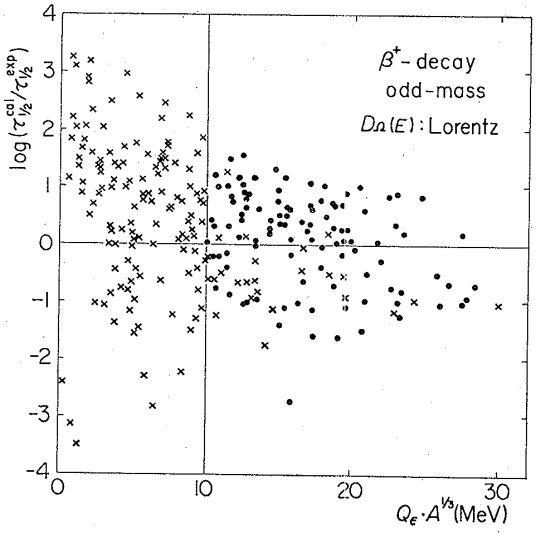

(d)

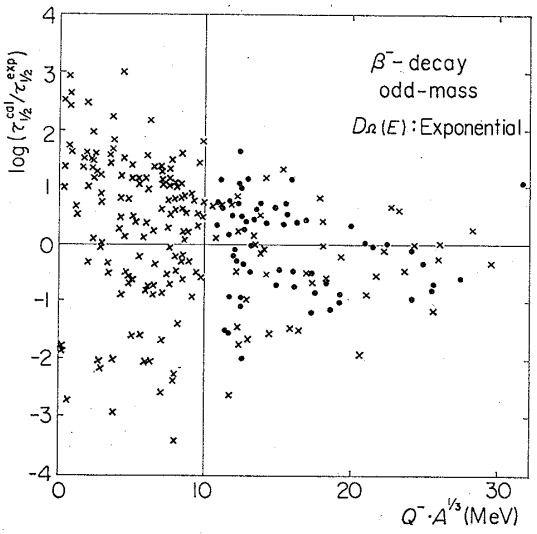

(e)

Fig. 4. Comparison of the calculated half-lives $\tau_{1/2}^{\text{cal}}$ with the experimental ones $\tau_{1/2}^{\text{exp}}$ for odd-mass nuclei in the model of § 4 (see Table I). The abscissa, $Q\cdot A^{1/3}$, is a sort of measure of the number of final levels, and the second criterion (47) is shown by vertical lines, $Q\cdot A^{1/3}=10$. Circles correspond to the qualified nuclei and crosses to the unqualified.

n-th nucleus, respectively.

We introduce the mismatch factor defined as

$$\eta = 10^{\sqrt{S/N_0}}, \tag{49}$$

which gives the average deviation of the ratio $\tau_{1/2}^{\rm cal}/\tau_{1/2}^{\rm exp}$ from unity.

The values of the parameter $\sigma_{\rm N}$ obtained by applying the above method to odd-mass nuclei are given in Table I. When there are two local minima of S, we take the one corresponding to the smaller value of $\sigma_{\rm N}$ though the other gives even better results in some cases (cf. Fig. 11). In § 6, we discuss the second minimum corresponding to the larger value of $\sigma_{\rm N}$.

The calculated half-lives are compared with the experimental ones in Fig. 4 for several optimal cases. Although the agreements of individual data are not very good, the situation is encouraging because the plots are distributed statistically around the axis of $\tau_{1/2}^{\rm cal}/\tau_{1/2}^{\rm exp}=1$. In this point, our results are more favorable than those of the usual single-particle calculations. In particular, the gross theory gives better results for nuclei with relatively high Q-values in accordance with the criterion II, and the numerical results depend little on Z and A.

Table I. Best-fit values of the width parameters, $\sigma_{\rm N}$ and $\Gamma_{\rm N}/2$, and the mismatch factor η (Eq. (49)) in the model of § 4. Only odd-mass nuclei are used. N_0 is the total number of qualified nuclei.

$D_{\rm GT}(E)$	β^+-decay		β^--decay	
	$N_0=105$		$N_0=60$	
	$\sigma_{\rm N}$(MeV)	η	$\sigma_{\rm N}$(MeV)	η
Gaussian	5.0	5.6	6.0	6.7
Exponential	4.4	5.8	5.5	6.4
Modified-Lorentz	5.4 ($\gamma=6$)	6.1	6.8 ($\gamma=7$)	6.3
Lorentz	$\Gamma_{\rm N}/2=1.7$	6.7	$\Gamma_{\rm N}/2=2.2$	6.4

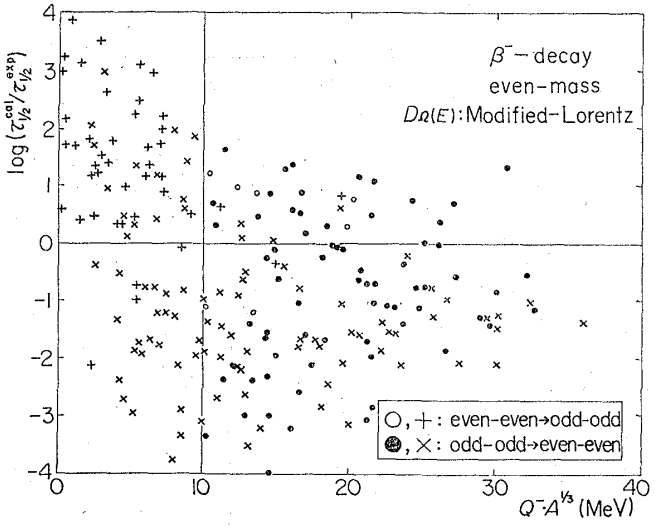

Fig. 5. A part of the results for even-mass nuclei in the model of § 4. For $\sigma_{\rm N}$ and γ the values for odd-mass nuclei (see Table I) are used. See also the caption of Fig. 4.

The results for even-mass nuclei are shown in Fig. 5 in the case of the modified-Lorentz

type with the values of σ_N and γ given in Table I. It is found that $\tau_{1/2}^{cal} \lessapprox \tau_{1/2}^{exp}$ for the transitions from odd-odd to even-even nuclei, and $\tau_{1/2}^{cal} \gtrapprox \tau_{1/2}^{exp}$ for the transitions from even-even to odd-odd nuclei. These tendencies can be understood by the following considerations. For the transition from odd-odd to even-even nucleus, the number of the final levels is rather small compared with its high Q-value, compelling us to overestimate the decay rate as far as the parameter value for odd-mass nuclei is used. Conversely, for the transition from even-even to odd-odd nucleus the number of the final levels is rather large compared with its low Q-value, making the calculated decay rate too low. These difficulties are overcome in the next section by considering the even-odd mass difference.

§ 5. Calculations in consideration of even-odd mass difference

If we try to deal with even-mass nuclei and odd-mass ones on the same footing, the consideration of the pairing effect or the even-odd mass difference is necessary. In treating the pairing force the BCS theory[21] has been applied successfully.[22] However, the gross theory does not deal with the wave function explicitly, so that we pay attention only to the gap in the energy spectrum caused by the pairing interaction.

Although the pairing theory predicts a quasi-particle spectrum of $\sqrt{\varepsilon'^2+\Delta^2}$ type where ε' is the energy of unpaired single particle, we use a simplified spectrum. We assume that the single-nucleon states with energies between ε_F and $\varepsilon_F+\Delta$ and between ε_F and $\varepsilon_F-\Delta$ (2Δ is the gap) are pushed up and down respectively by the pairing force and that the pushed levels are piled up at the boundaries of the gap in the form of δ-function. Thus the single-nucleons in the parent nucleus have the configuration indicated in Figs. 6 and 7. For Δ, we use the so-called δ-term in the mass formula approximated as[23]

$$\Delta = 11.2A^{-1/2}\ \text{MeV}, \tag{50}$$

in which no distinction is made between the energy gaps in the single-proton

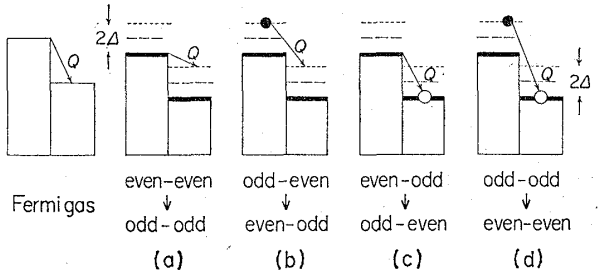

Fig. 6. The single-nucleon states in the parent nucleus in consideration of the even-odd mass difference for four types of transitions. The pairing force pushes up and down the single-nucleon states near the Fermi surfaces resulting the energy gaps of 2Δ. The thick lines represent the states piled up in the form of δ-function. ● : last odd particle, ○ : hole.

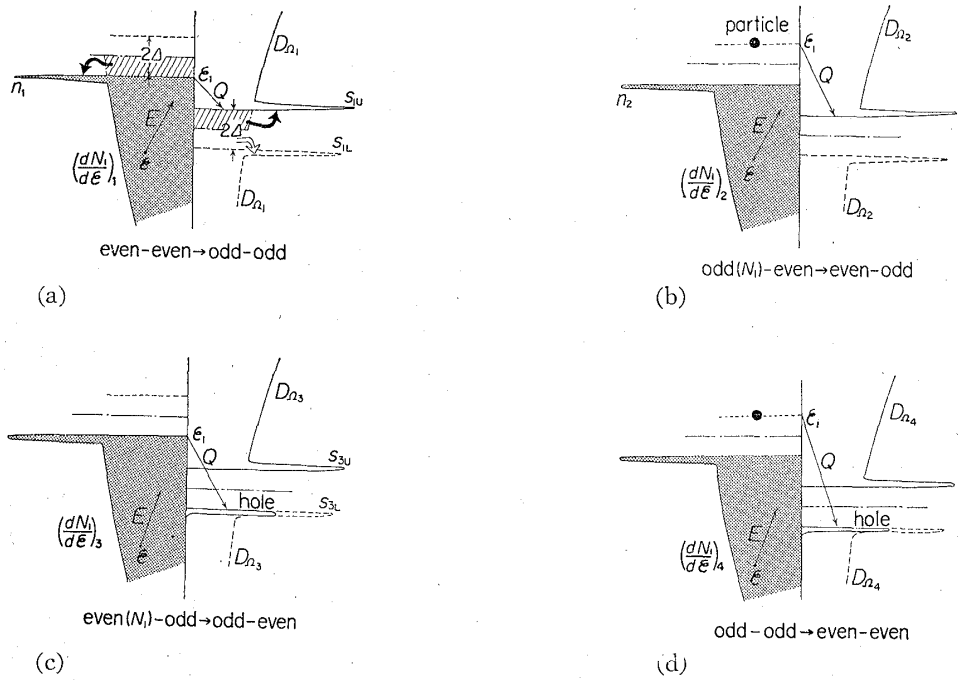

Fig. 7. Schematic illustration of the model of § 5. $dN_1/d\varepsilon$ is shown in the left halves and $D_\varrho(E,\varepsilon)$ is shown in the right halves. Owing to the Pauli principle actual transitions occur to the parts of D_ϱ drawn by solid lines.

and single-neutron states.

In this simplified description, the explicit forms for the total decay rates can be derived as follows.

1. *Transition from even-even to odd-odd nucleus*

From Fig. 7(a), we get $dN_1/d\varepsilon$ as

$$\left(\frac{dN_1}{d\varepsilon}\right)_1 = \left(\frac{dN_1}{d\varepsilon}\right)_0 \cdot h_1(\varepsilon) + n_1 \cdot \delta(\varepsilon - \varepsilon_1), \tag{51}$$

with

$$h_1(\varepsilon) = \begin{cases} 1 & \text{for } \varepsilon_1 + \Delta - \varepsilon_F \leqq \varepsilon \leqq \varepsilon_1, \\ 0 & \text{otherwise.} \end{cases} \tag{52}$$

Here, $\delta(x)$ is the δ-function, and $(dN_1/d\varepsilon)_0$ is the number density in the Fermi gas model given by Eq. (26) with $\varepsilon_{\min} = \varepsilon_1 + \Delta - \varepsilon_F$. The number of the nucleons piled up on the uppermost level ($\varepsilon = \varepsilon_1$) is equal to that of the nucleons which would lie between $\varepsilon = \varepsilon_1$ and $\varepsilon_1 + \Delta$ if there were no gap. Namely,

$$n_1 = \int_{\varepsilon_1}^{\varepsilon_1 + \Delta} \left(\frac{dN_1}{d\varepsilon}\right)_0 d\varepsilon . \tag{53}$$

In a similar way, $D_\varrho(E)$ is also modified by the gap of the single-nucleon levels in the final nucleus. The part of $D_\varrho(E)$, which would fall in the upper

(lower) half of the gap region if the gap did not exist, is piled up at the upper (lower) end of this region. Thus, from the right side of Fig. 7(a), we get as one of the simplest forms of $D_{\varrho}(E, \varepsilon)$,

$$D_{\varrho 1}=D_{\varrho_0}(E)\cdot g_1(\varepsilon+E)+s_{1\mathrm{L}}(\varepsilon)\cdot\delta(\varepsilon+E-\varepsilon_1+Q+2\Delta)+s_{1\mathrm{U}}(\varepsilon)\cdot\delta(\varepsilon+E-\varepsilon_1+Q), \tag{54}$$

with

$$g_1(\varepsilon+E)=\begin{cases}0 & \text{for } \varepsilon_1-Q-2\Delta\leqq\varepsilon+E\leqq\varepsilon_1-Q,\\ 1 & \text{otherwise.}\end{cases} \tag{55}$$

Here, $D_{\varrho_0}(E)$ is the trial function introduced in Eqs. (33), (36) and (39)$\sim$(44), and

$$s_{1\mathrm{L}}(\varepsilon)=\int_{\varepsilon_1-Q-2\Delta-\varepsilon}^{\varepsilon_1-Q-\Delta-\varepsilon}D_{\varrho_0}(E)\,dE \tag{56}$$

and

$$s_{1\mathrm{U}}(\varepsilon)=\int_{\varepsilon_1-Q-\Delta-\varepsilon}^{\varepsilon_1-Q-\varepsilon}D_{\varrho_0}(E)\,dE\,. \tag{57}$$

For convenience we express the Pauli principle by using the weight function $W(E, \varepsilon)$ in Eq. (22)

$$W_1(E, \varepsilon)=\begin{cases}1 & \text{for } \varepsilon+E\geqq\varepsilon_1-Q,\\ 0 & \text{for } \varepsilon+E<\varepsilon_1-Q.\end{cases} \tag{58}$$

Substituting $(dN_1/d\varepsilon)_1$ for $dN_1/d\varepsilon$, $D_{\varrho 1}$ for $D_{\varrho}(E, \varepsilon)$ and $W_1(E, \varepsilon)$ for $W(E, \varepsilon)$ in Eq. (25), we get the expression for the total decay rate λ as

$$\begin{aligned}\lambda_1=\lambda_1(N_1, Q, \varepsilon_{\mathrm{F}}(N_1))\\ \equiv\frac{m_e{}^5c^4}{2\pi^3\hbar^7}\Bigg[&N_1\int_{-Q}^{0}\left\{1-\left(1-\frac{Q+E+\Delta}{\varepsilon_{\mathrm{F}}(N_1)}\right)^{3/2}\right\}G_0{}^2D_0(E)f(-E)\,dE\\ &+\frac{3N_1}{2\varepsilon_{\mathrm{F}}(N_1)}\int_{-Q}^{0}\left(1-\frac{Q+E+\Delta}{\varepsilon_{\mathrm{F}}(N_1)}\right)^{1/2}\left\{\int_{E-\Delta}^{E}G_0{}^2D_0(E')\,dE'\right\}f(-E)\,dE\\ &+N_1\left\{1-\left(1-\frac{\Delta}{\varepsilon_{\mathrm{F}}(N_1)}\right)^{3/2}\right\}f(Q)\int_{-Q-\Delta}^{-Q}G_0{}^2D_0(E)\,dE\Bigg],\end{aligned} \tag{59}$$

with

$$G_0{}^2D_0(E)\equiv|G_{\mathrm{F}}|^2D_{\mathrm{F}}(E)+3|G_{\mathrm{GT}}|^2D_{\mathrm{GT}}(E). \tag{60}$$

2. *Transition between odd-mass nuclei* (odd N_1)

From Fig. 7(b), we get $dN_1/d\varepsilon$ as

$$\left(\frac{dN_1}{d\varepsilon}\right)_2=\left(\frac{d(N_1-1)}{d\varepsilon}\right)_0\cdot h_2(\varepsilon)+n_2\cdot\delta(\varepsilon-\varepsilon_1+2\Delta)+\delta(\varepsilon-\varepsilon_1), \tag{61}$$

with

$$h_2(\varepsilon)=\begin{cases}1 & \text{for } \varepsilon_1-\Delta-\varepsilon_F\leqq\varepsilon\leqq\varepsilon_1-2\Delta,\\ 0 & \text{otherwise}\end{cases} \tag{62}$$

and

$$n_2=\int_{\varepsilon_1-2\Delta}^{\varepsilon_1-\Delta}\left(\frac{d(N_1-1)}{d\varepsilon}\right)_0 d\varepsilon. \tag{63}$$

Here, $(d(N_1-1)/d\varepsilon)_0$ is given by Eqs. (26)$\sim$(28) in which ε_1 is replaced by $\varepsilon_1-\Delta$ and N_1 replaced by N_1-1. The last term of Eq. (61) represents the last nucleon in Fig. 7(b). This nucleon is assumed to lie at the top of the energy gap ($\varepsilon=\varepsilon_1$) in the form of δ-function although there may be no sufficient room. Actually, the number of single-nucleon states at $\varepsilon=\varepsilon_1$ is given by

$$n_2'=\int_{\varepsilon_1-\Delta}^{\varepsilon_1}\left(\frac{d(N_1-1)}{d\varepsilon}\right)_0 d\varepsilon, \tag{64}$$

and, as far as Eqs. (30) and (50) are used, $n_2'<1$ for $A\lesssim 50$; e.g. $n_2'\approx 0.7$ for $A=20$. This means that the single-nucleon state at $\varepsilon=\varepsilon_1$ cannot accommodate one nucleon in the case of relatively light nuclei. This inconsistency might be removed if some fraction of the upper states with $\varepsilon>\varepsilon_1$ is shifted down to $\varepsilon=\varepsilon_1$ to fill up the above-mentioned shortage.

The expressions for $D_Q(E,\varepsilon)$ and $W(E,\varepsilon)$ in case 1 are also valid in this type of transition;

$$D_{Q2}=D_{Q1}, \tag{65}$$

and

$$W_2=W_1. \tag{66}$$

Now, the total decay rate λ is given by

$$\lambda_2=\lambda_1(N_1-1,\,Q-2\Delta,\,\varepsilon_F(N_1-1))+\lambda_{2p}(Q), \tag{67}$$

where the last term

$$\lambda_{2p}(Q)\equiv\frac{m_e^5c^4}{2\pi^3\hbar^7}\left[\int_{-Q}^{0}G_0^2D_0(E)f(-E)\,dE+f(Q)\int_{-Q-\Delta}^{-Q}G_0^2D_0(E)\,dE\right] \tag{68}$$

is the decay rate of the last odd nucleon.

3. *Transition between odd-mass nuclei (even N_1)*

From Fig. 7(c), we get

$$\left(\frac{dN_1}{d\varepsilon}\right)_3 = \left(\frac{dN_1}{d\varepsilon}\right)_1, \tag{69}$$

and

$$D_{\varrho 3} = D_{\varrho 0}(E)\cdot g_3(\varepsilon+E) + s_{3\mathrm{L}}(\varepsilon)\cdot\delta(\varepsilon+E-\varepsilon_1+Q) + s_{3\mathrm{U}}(\varepsilon)\cdot\delta(\varepsilon+E-\varepsilon_1+Q-2\Delta), \tag{70}$$

with

$$g_3(\varepsilon+E) = g_1(\varepsilon+E-2\Delta) = \begin{cases} 0 & \text{for } \varepsilon_1-Q\leqq\varepsilon+E\leqq\varepsilon_1-Q+2\Delta, \\ 1 & \text{otherwise,} \end{cases} \tag{71}$$

$$s_{3\mathrm{L}}(\varepsilon) = s_{1\mathrm{L}}(\varepsilon-2\Delta), \tag{72}$$

and

$$s_{3\mathrm{U}}(\varepsilon) = s_{1\mathrm{U}}(\varepsilon-2\Delta). \tag{73}$$

In this case, the Pauli principle can be expressed in terms of the weight function as

$$W_3(E,\varepsilon) = \begin{cases} 1 & \text{for } \varepsilon+E\geqq\varepsilon_1-Q+2\Delta, \\ 1/n_3 & \text{for } \varepsilon+E=\varepsilon_1-Q, \\ 0 & \text{otherwise.} \end{cases} \tag{74}$$

Here, n_3 is the number of the final single-nucleon states which would lie in the lower half of the gap region if there were no gap, and is given by

$$n_3 = \int_{\varepsilon_1-Q}^{\varepsilon_1-Q+\Delta} \left(\frac{dN_2}{d\varepsilon}\right)_0 d\varepsilon. \tag{75}$$

Here, $(dN_2/d\varepsilon)_0$ is the number density of neutron and proton in the final nucleus for β^+- and β^--decays, respectively, and is evaluated by the Fermi gas model similarly to $(dN_1/d\varepsilon)_0$. Then, the factor $1/n_3$ in the weight function (74) indicates that only one single-nucleon hole in the n_3 final states is available for the transition. Here we assume that the hole always exists though this assumption may lead to the inconsistency that n_3 is less than unity for relatively light nuclei. This situation is similar to that of the last odd nucleon in the case of odd-N_1 odd-mass nuclei, and a similar solution in the interpretation might be possible.

The total decay rate λ is given by

$$\lambda_3 = \lambda_1(N_1, Q-2\Delta, \varepsilon_{\mathrm{F}}(N_1)) + \lambda_{3\mathrm{h}}(N_1, Q, \varepsilon_{\mathrm{F}}(N_1)), \tag{76}$$

where the last term

$$\lambda_{3h}(N_1, Q, \varepsilon_F(N_1))$$

$$= \frac{m_e^5 c^4}{2\pi^3 \hbar^7}\left[\left(1\Big/N_2\left\{1-\left(1-\frac{\Delta}{\varepsilon_F(N_2)}\right)^{3/2}\right\}\right)\frac{3N_1}{2\varepsilon_F(N_1)}\int_{-Q}^{0}\left\{\left(1-\frac{Q+E+\Delta}{\varepsilon_F(N_1)}\right)^{1/2} f(-E)\right.\right.$$

$$\left.\times\int_{E}^{E+\Delta} G_0^2 D_0(E')\,dE'\right\}dE + f(Q)\,N_1\left\{1-\left(1-\frac{\Delta}{\varepsilon_F(N_1)}\right)^{3/2}\right\}$$

$$\left.\times\left(1\Big/N_2\left\{1-\left(1-\frac{\Delta}{\varepsilon_F(N_2)}\right)^{3/2}\right\}\right)\int_{-Q}^{-Q+\Delta} G_0^2 D_0(E)\,dE\right] \qquad (77)$$

is the decay rate to the hole state. Here, N_2 is the total neutron (proton) number for $\beta^+(\beta^-)$-decay in the daughter nucleus. When $N_1=N_2$, Eq. (77) is reduced to the expression nearly but not exactly equal to Eq. (68).

4. *Transition from odd-odd to even-even nucleus*

From Fig. 7(d), we get

Table II. Best-fit values of the width parameter, σ_N and $\Gamma_N/2$, and the mismatch factor η (Eq. (49)) in the model of § 5. N_0 is the total number of qualified nuclei.

$D_{GT}(E)$	Z-N (parent)	β^+-decay			β^--decay		
		N_0	σ_N(MeV)	η	N_0	σ_N(MeV)	η
Gaussian	even-even	19	4.0	5.9	7	4.5	12.9
	odd-even	50	4.0	6.3	22	5.1	6.5
	even-odd	55	4.9	5.9	38	5.1	9.4
	odd-odd	102	4.3	42.8	72	5.0	45.5
Exponential	even-even	19	2.5	7.4	7	3.3	10.0
	odd-even	50	2.7	5.4	22	4.3	6.2
	even-odd	55	3.8	4.8	38	3.7	6.8
	odd-odd	102	2.5	31.8	72	3.2	32.0
Modified-Lorentz ($\gamma=100$)	even-even	19	4.7	9.8	7	7.5	9.3
	odd-even	50	6.3	5.4	22	9.0	6.2
	even-odd	55	9.0	4.4	38	7.0	5.8
	odd-odd	102	4.7	20.9	72	4.5	26.3
Lorentz	even-even	19	$\Gamma_N/2=0.3$	10.0	7	$\Gamma_N/2=0.6$	9.2
	odd-even	50	$\Gamma_N/2=0.5$	5.4	22	$\Gamma_N/2=0.9$	6.2
	even-odd	55	$\Gamma_N/2=0.9$	4.4	38	$\Gamma_N/2=0.5$	5.8
	odd-odd	102	$\Gamma_N/2=0.3$	21.0	72	$\Gamma_N/2=0.3$	27.0

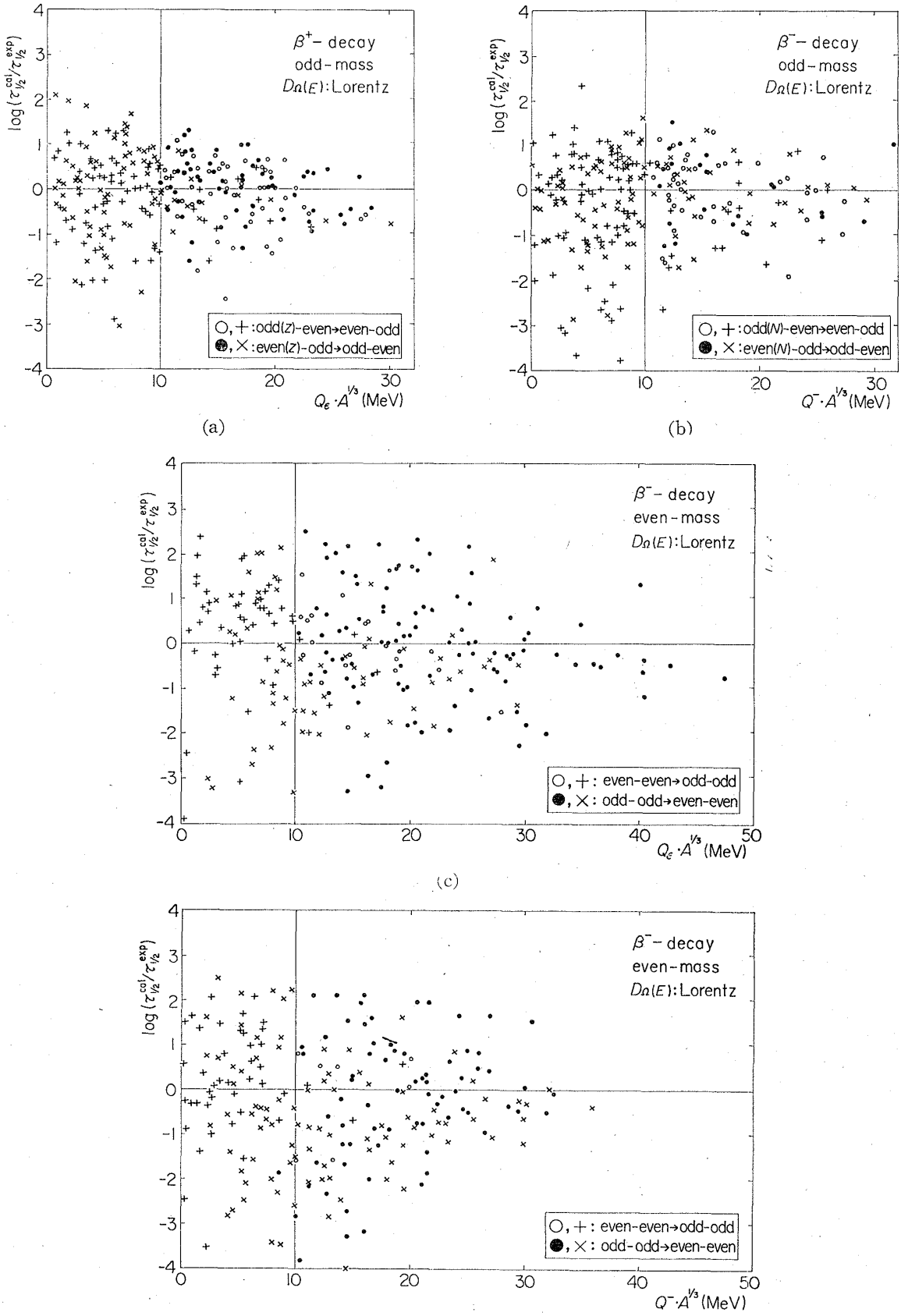

Fig. 8. Comparison of the calculated half-lives $\tau_{1/2}^{\text{cal}}$ with the experimental ones $\tau_{1/2}^{\text{exp}}$ in the model of § 5 (see Table II). See also the caption of Fig. 4.

$$\left(\frac{dN_1}{d\varepsilon}\right)_4 = \left(\frac{dN_1}{d\varepsilon}\right)_2, \tag{78}$$

$$D_{Q4} = D_{Q3} \tag{79}$$

and

$$W_4 = W_3 . \tag{80}$$

Then, the total decay rate λ is given by

$$\lambda_4 = \lambda_1(N_1-1, Q-4\Delta, \varepsilon_F(N_1-1)) + \lambda_{2p}(Q-2\Delta) + \lambda_{3h}(N_1-1, Q-2\Delta, \varepsilon_F(N_1-1)) + \lambda_{4ph}(Q), \tag{81}$$

where the last term

$$\lambda_{4ph}(Q) \equiv \frac{m_e^5 c^4}{2\pi^3\hbar^7}\left(1\Big/N_2\left\{1-\left(1-\frac{\Delta}{\varepsilon_F(N_2)}\right)^{3/2}\right\}\right) f(Q)\left\{\int_{-Q}^{-Q+\Delta} G_0^2 D_0(E)\,dE\right\} \tag{82}$$

is the decay rate of the last odd nucleon to the hole state.

Some of the numerical results are given in Table II and Fig. 8. When there are two local minima of S (Eq. (48)), we take only the smaller value of σ_N as has been done in § 4. The important point in the results of this section is that no systematic difference is seen between the even-mass and odd-mass nuclei. However, the agreement with experiment is not very good, especially for the transitions from odd-odd to even-even nuclei. On this point, we discuss in the next section.

§ 6. Discussion

Our theory is characterized by the gross approximation of § 2 and the gross model of § 3. The gross approximation becomes better according as the number of final levels increases. However, in order to get reliable statistics, we have been forced to utilize a rather large number of nuclei with few final states. The nuclei that lie far from the β-stability line have large Q-values and many final states. Therefore, the β^+-decays of such nuclei are useful for the investigation of the peak of the distribution function D_Q, and the β^--decays are useful for the study of its tail. We expect that more decays with large Q-values which enable us to refine the analysis will be discovered in the near future.

In the model of § 3 the quantum-mechanical interference is neglected. If there is a common part between the residual interaction Hamiltonian and the positive-definite operator $\sum_{l,m}\omega_l^\dagger\omega_m$ (see, § 2) with the same sign, then $\langle\Psi_I|\sum_{l,m}\omega_l^\dagger\omega_m|\Psi_I\rangle$ and the transition rate tend to become smaller because the expectation value of the Hamiltonian is minimum in the ground state. On the other hand, if there is a common part with opposite signs, the transition rate tends to become larger. In the case of the allowed β-decay, there seems to be

no marked enhancement or reduction. Although the quantitative evaluation of these effects does not seem easy, it might be possible by the use of the wave function of the form $\Psi = F\Phi$, where Φ is the model wave function in the single-nucleon picture and F is the correlation function. If we replace the operators such as $\Omega^\dagger\Omega$ and $\Omega^\dagger[H, \Omega]$ in Eqs. (4) and (5) by the operators $F^\dagger\Omega^\dagger\Omega F$ and $F^\dagger\Omega^\dagger[H, \Omega]F$, we might proceed in a way similar to the previous sections.

In our calculation, we have used the β-decay Q-values between ground states. However, this choice is not adequate in such a case where the allowed transitions go only to highly excited states. In this case, the decay rate is apt to be overestimated. In Fig. 9, we plot $\tau_{1/2}^{\mathrm{cal}}/\tau_{1/2}^{\mathrm{exp}}$ for some even-mass nuclei against the quantity

$$\left[\frac{f_a}{f_{gs}}\left(\frac{Q_a}{Q_{gs}}\right)^2\right] \tag{83}$$

on the log-log scale. Here, Q_{gs} is the ground-state Q-value and Q_a is the Q-value for the lowest final state among those fed by allowed transitions. The values of f-function f_{gs} and f_a correspond to Q_{gs} and Q_a, respectively. The reason for the introduction of the factor $(Q_a/Q_{gs})^2$ in (83) is that the decay rate is closely related to the area of the tail of $|M_\varrho(E)|^2$ and this area is approximately proportional to the square of the Q-value in the case of no pairing (see Fig. 2). This factor might be applied even to the case with the pairing correction if we smooth out the singularity of $|M_\varrho(E)|^2$. The approximate proportionality of the ratio $(\tau_{1/2}^{\mathrm{cal}}/\tau_{1/2}^{\mathrm{exp}})$ to the quantity (83) is seen in Fig. 9 in which the pairing correction is included, and it suggests that a more appropriate choice of the Q-value will give better agreement with experiment, in particular, for the transitions from odd-odd to even-even nuclei.

Furthermore, better agreement with experiment is expected if, instead of the half-life, the distribution of comparative half-lives (fi-values) over final states is used in the analysis of experimental data, because the differences of our results with experimental data are largely due to the drastic energy dependence of the f-function. However, the process of analysis will become much more involved.

From Fig. 2 it is to be expected that the β^--decay is more hindered than the β^+-decay and, in fact, this tendency is seen in the experimental data.[24] The small differences between σ_N's obtained for β^+- and β^--decays (cf. Tables I and II) are probably ascribable to some statistical reason.

It is hard to determine the best type of the distribution function $D_\varrho(E)$ from the above analysis only, because similar results have been obtained with the four trial forms as seen in Fig. 4. Investigations of special cases (e.g. superallowed transitions, pure Fermi transitions) and of quantities other than the half-life may be helpful for the discrimination among types.

The effect of the Pauli principle is included in the lower limit of the integration domain of (17). No apparent inadequacy of this treatment is seen in

the results of this paper. It should be noted that, as far as the transitions with low Q-values are concerned, the method of treating the Pauli principle affects the numerical results more seriously than the uncertainty in the form of $D_\varrho(E)$ does.

We have assumed that the surfaces of the single-nucleon levels are flat. However, our model might be valid even in the case with diffuse surfaces provided that the diffuseness and the transition are such as shown in Fig. 10.

In our calculation there are other kinds of flexibilities and uncertainties such as the value of the effective mass and the method for treating the pairing correction. As for the latter, we can substitute some other function for the δ-function, and also can define the D_ϱ function from the continuous $D_{\varrho 0}(E)$ function in a different way. However, these uncertainties do not seem to have important effect on our present rough analysis. The experimental data[19),20)] used in our analysis are not completely up-to-date, but their possible errors will not be so large as to change the results appreciably.

The numerical results in §§ 4 and 5 are consistent with the "persistent" supermultiplet structure expected in the Gamow-Teller transition.[10)] In particular, the value of a few MeV obtained as the energy spread of $D_{\mathrm{GT}}(E)$ is in nice agreement with that estimated from the spin-orbit splitting in the shell model. However, as noted in § 4 the quantity S (Eq. (48)) experiences the second minimum when the energy spread becomes much wider. The existence of these second minima which have been neglected in making Tables I and II is now shown in Fig. 11. The behavior of the curves of Fig. 11 can be qualitatively understood as follows. When the energy spread of $D_{\mathrm{GT}}(E)$ is very small, the calculated decay rates are generally too low because the tail of the distribution responsible for the actual decay is too small. As the energy spread increases, the decay rates reach their local optimal values. A further increase of energy spread makes the decay rates too high, but beyond a certain energy spread the decay rates begin to decrease because the distribution is so much spread that its magnitudes at the energy values relevant to the actual decay start diminishing. Then, the decay rates pass the second local optimal values, and approach nil except for the modified-Lorentz type. In the case of the modified-Lorentz type, S (or η) converges to a value as $\sigma_{\mathrm{N}}\to\infty$, and the second minimum may not appear. The fact that the energy spreads of these second minima are extremely large indicates that the persistent supermultiplet is completely broken down there. It is hard to decide which minimum is more reasonable from the above analysis only, but other kinds of analyses might be helpful for the discrimination.

In closing this paper, we discuss on some relating problems briefly.

In the above calculation, the Fermi transition makes little contribution because it is masked behind the Gamow-Teller transition. It will be interesting to investigate the Fermi transition separately. In this case, it will be necessary to treat the detailed structure of $D_{\mathrm{F}}(E, \varepsilon)$ and the Coulomb displacement energy

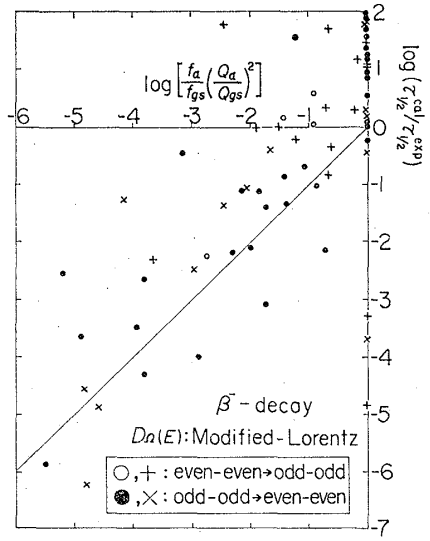

Fig. 9. Ratios of the calculated half-lives of even-mass nuclei to the experimental ones are plotted against the quantity (83) on the log-log scale. Circles correspond to the qualified nuclei and crosses to the unqualified. The values of the parameters σ_N and γ are given in Table II.

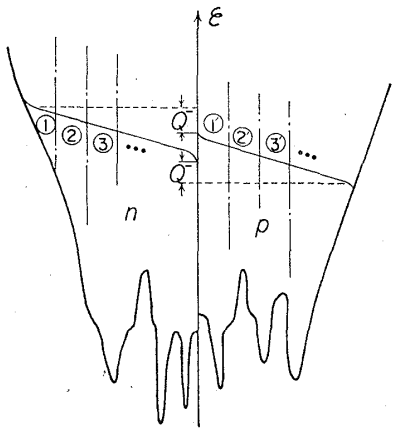

Fig. 10. Diffuse surfaces for which our model might be valid are illustrated for β^--decay. The surfaces for neutron and proton have the same shape and the vertical distance between them is equal to Q^-. The neutron in the i-th column decays into i'-th one above the proton surface.

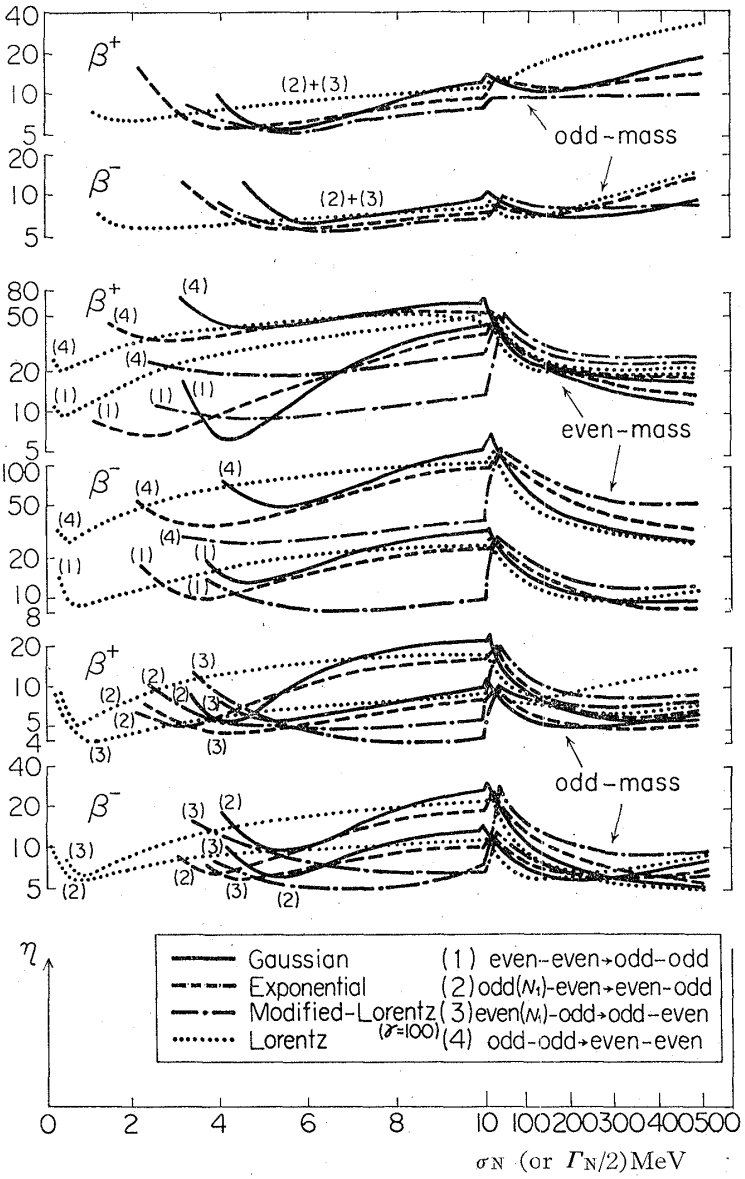

Fig. 11. Existence of two local "best" fits is shown. The mismatch foctor η (Eq. (49)) is plotted against the width parameter, σ_N or $\Gamma_N/2$. Two groups of drawings on the top are obtained in the model of § 4 for odd-mass nuclei and the others are obtained in the model of § 5 for nuclei including even-mass ones.

carefully and to take into account the higher-order matrix elements.[25]

One of the direct applications of the gross theory of β-decay is that to the composite spectrum of emitted electrons. The electron spectrum from fission fragments can be treated in a similar way.

Another possible application is that to delayed neutrons or protons.*) The energy spectrum of the emitted neutrons or protons and the percentage of the particle emission can be easily calculated by the gross theory.

Similarly, the mean excitation energy after β-decay or the average of the total γ-ray energy per decay can be calculated.

The inclusion of the 1-st forbidden transition will make the results more reliable, especially for heavy nuclei. In this case, the interference effect among various nuclear matrix elements will be important. In order to take into account this effect, quantities of the form $\langle \Phi_{\Omega 1} | (H-E_I)^n | \Phi_{\Omega 2} \rangle$ $(n=0, 1, 2)$ must be estimated. These kinds of quantities are also important in the study of angular correlations. We cannot say at present whether the gross theory is successfully applicable to these quantities or not.

The gross theory will be applicable to any process described by the sum of single-particle operators as far as the number of final states is large. For example, the photoreaction, the γ-decay, the μ-capture and possibly the π-capture come under this category.

Acknowledgments

This work has been carried out as a part of the annual research project for "Nuclear Structure and Weak Interaction" in 1965~68 of the Research Institute for Fundamental Physics, Kyoto University. The authors are greatly indebted to Professors M. Morita, A. Fujii, J. I. Fujita and Dr. K. Ikeda for their stimulating discussions.

Thanks are also due to Messrs. K. Ohshima, T. Kodama and S. Koyama for valuable discussions. The assistance afforded by two of them (K.O. and T.K.) in preparing the approximate formulas for the integrated Fermi function has been very helpful.

The numerical calculations were made with the aid of HITAC 5020E at The Computer Center, Tokyo University and NEAC 2203 at The Electronic Computation Center, Waseda University.

Appendix A

Description of the gross theory in the second-quantization formalism

We investigate the meaning of our model of § 3 in more detail, taking the Fermi transition as an example. The second-quantization formalism is suitable

*) The authors would like to express their thanks to Professor H. Morinaga who suggested the possibility of this application.

for this purpose because the "single-nucleon state" plays an important role in the model.

The Coulomb energy plus the neutron-hydrogen mass difference is written as

$$H_{\mathrm{C}}=\tfrac{1}{4}\sum_{stpq}\mathcal{V}_{stpq}a_s^{\dagger}a_t^{\dagger}a_pa_q+\Delta_{\mathrm{nH}}\sum_r b_r^{\dagger}b_r\,, \tag{A1}$$

where $a^{\dagger}$ and a are the creation and annihilation operators of proton, $b^{\dagger}$ and b are those of neutron, and

$$\mathcal{V}_{stpq}=\iint\left[\phi_s^*(1)\,\phi_t^*(2)\frac{e^2}{r_{12}}\phi_p(2)\,\phi_q(1)-\phi_s^*(2)\,\phi_t^*(1)\frac{e^2}{r_{12}}\phi_p(2)\,\phi_q(1)\right]d\tau_1d\tau_2\,, \tag{A2}$$

$$\mathcal{V}_{stpq}=-\mathcal{V}_{tspq}=-\mathcal{V}_{stqp}=\mathcal{V}_{tsqp}\,. \tag{A3}$$

For the β^- Fermi transition,

$$\Omega=T_+=\sum_m a_m^{\dagger}b_m \tag{A4}$$

and

$$[H_{\mathrm{C}},\,T_+]=\tfrac{1}{2}\sum_{stpq}\mathcal{V}_{stpq}a_s^{\dagger}a_t^{\dagger}a_pb_q-\Delta_{\mathrm{nH}}\sum_r a_r^{\dagger}b_r\,. \tag{A5}$$

Now, we assume that $\{\phi_i\}$ is a set of base functions appropriate for describing neutrons in the single-nucleon picture. We introduce another set of base functions $\{\phi_j'\}$ appropriate to protons, and designate the corresponding creation and annihilation operators by $\alpha^{\dagger}$, α and $\beta^{\dagger}$, β. The proton wave function

$$\psi^{(p)}(\boldsymbol{r})=\sum_i\phi_i(\boldsymbol{r})\,a_i \tag{A6}$$

is transformed into

$$\psi^{(p)}(\boldsymbol{r})=\sum_j\phi_j'(\boldsymbol{r})\,\alpha_j \tag{A7}$$

by a unitary transformation:

$$a_i=\sum_j d_{ij}\alpha_j\,, \tag{A8}$$

$$\sum_i d_{ij}^*d_{ik}=\delta_{jk}\,, \tag{A9}$$

$$\phi_j'(\boldsymbol{r})=\sum_i d_{ij}\phi_i(\boldsymbol{r})\,. \tag{A10}$$

Here, the matrix (d_{ij}) represents the overlap between the neutron base functions $\{\phi_i\}$ and the proton ones $\{\phi_j'\}$.

The quantities appearing in Eqs. (4)$\sim$(6) can be written as

$$\langle\Psi_{\mathrm{I}}|T_-T_+|\Psi_{\mathrm{I}}\rangle=\langle\Psi_{\mathrm{I}}|\Big(\sum_{q'}\sum_i d_{q'i}b_{q'}^{\dagger}\alpha_i\Big)\Big(\sum_q\sum_j d_{qj}^*\alpha_j^{\dagger}b_q\Big)|\Psi_{\mathrm{I}}\rangle\,, \tag{A11}$$

$$\langle\Psi_{\mathrm{I}}|T_-[H_{\mathrm{C}},\,T_+]|\Psi_{\mathrm{I}}\rangle=\langle\Psi_{\mathrm{I}}|\Big(\sum_{q'}\sum_i d_{q'i}b_{q'}^{\dagger}\alpha_i\Big)\Big(\sum_q\sum_{j,k}\mathcal{U}_{jkkq}\alpha_j^{\dagger}\alpha_k^{\dagger}\alpha_kb_q\Big)|\Psi_{\mathrm{I}}\rangle$$

$$+\tfrac{1}{2}\langle\Psi_{\rm I}|\Big(\sum_{q'}\sum_{i} d_{q'i}b_{q'}^{\dagger}\alpha_i\Big)\Big(\sum_{q}\sum_{\substack{j,k\\ l(\neq j,k)}} \mathcal{U}_{jklq}\alpha_j^{\dagger}\alpha_k^{\dagger}\alpha_l b_q\Big)|\Psi_{\rm I}\rangle$$

$$-\Delta_{\rm nH}\langle\Psi_{\rm I}|T_-T_+|\Psi_{\rm I}\rangle\,, \tag{A12}$$

$$\langle\Psi_{\rm I}|[T_-,H_{\rm C}][H_{\rm C},T_+]|\Psi_{\rm I}\rangle$$
$$=\langle\Psi_{\rm I}|\sum_{q'}\sum_{i,n}\mathcal{U}^{*}_{inq'}b_{q'}^{\dagger}\alpha_n^{\dagger}\alpha_n\alpha_i\Big)\Big(\sum_{q}\sum_{j,k}\mathcal{U}_{jkkq}\alpha_j^{\dagger}\alpha_k^{\dagger}\alpha_k b_q\Big)|\Psi_{\rm I}\rangle$$
$$+\tfrac{1}{2}\langle\Psi_{\rm I}|\Big(\sum_{q'}\sum_{i,n}\mathcal{U}^{*}_{inq'}b_{q'}^{\dagger}\alpha_n^{\dagger}\alpha_n\alpha_i\Big)\Big(\sum_{q}\sum_{\substack{j,k\\ l(\neq j,k)}}\mathcal{U}_{jklq}\alpha_j^{\dagger}\alpha_k^{\dagger}\alpha_l b_q\Big)|\Psi_{\rm I}\rangle$$
$$+\tfrac{1}{2}\langle\Psi_{\rm I}|\Big(\sum_{q'}\sum_{\substack{i,n\\ l(\neq i,n)}}\mathcal{U}^{*}_{inlq'}b_{q'}^{\dagger}\alpha_l^{\dagger}\alpha_n\alpha_i\Big)\Big(\sum_{q}\sum_{j,k}\mathcal{U}_{jkkq}\alpha_j^{\dagger}\alpha_k^{\dagger}\alpha_k b_q\Big)|\Psi_{\rm I}\rangle$$
$$+\tfrac{1}{4}\langle\Psi_{\rm I}|\Big(\sum_{q'}\sum_{\substack{j',k'\\ l'(\neq j',k')}}\mathcal{U}^{*}_{j'k'l'q'}b_{q'}^{\dagger}\alpha_{l'}^{\dagger}\alpha_{k'}\alpha_{j'}\Big)\Big(\sum_{q}\sum_{\substack{j,k\\ l(\neq j,k)}}\mathcal{U}_{jklq}\alpha_j^{\dagger}\alpha_k^{\dagger}\alpha_l b_q\Big)|\Psi_{\rm I}\rangle$$
$$-2\Delta_{\rm nH}\langle\Psi_{\rm I}|T_-[H_{\rm C}^{0},T_+]|\Psi_{\rm I}\rangle+\Delta_{\rm nH}^{2}\langle\Psi_{\rm I}|T_-T_+|\Psi_{\rm I}\rangle\,, \tag{A13}$$

where

$$\mathcal{U}_{jklq}=\sum_{stp}\mathcal{V}_{stpq}d_{sj}^{*}d_{tk}^{*}d_{pl}\,, \tag{A14}$$

$$H_{\rm C}^{0}=H_{\rm C}-\Delta_{\rm nH}\sum_{r}b_r^{\dagger}b_r\,. \tag{A15}$$

The last two terms of Eq. (A13) vanish when the second moment is taken around the energy center of the Φ_Q-state.

Corresponding to the incoherent summation over single-nucleons in Eq. (17), the following two approximations are adopted:

$$\sum_{q',q}b_{q'}^{\dagger}b_q\longrightarrow\sum_{q}b_q^{\dagger}b_q\,, \tag{A16}$$

$$\sum_{i,j}\alpha_i\alpha_j^{\dagger}\longrightarrow\sum_{i}\alpha_i\alpha_i^{\dagger}. \tag{A17}$$

In these approximations, Equations (A11) $\sim$ (A13) become

$$\langle\Psi_{\rm I}|T_-T_+|\Psi_{\rm I}\rangle\approx\langle\Psi_{\rm I}|\sum_{q}b_q^{\dagger}\Big[\sum_{i}d_{qi}d_{qi}^{*}\alpha_i\alpha_i^{\dagger}\Big]b_q|\Psi_{\rm I}\rangle\,, \tag{A18}$$

$$\langle\Psi_{\rm I}|T_-[H_{\rm C},T_+]|\Psi_{\rm I}\rangle\approx\langle\Psi_{\rm I}|\sum_{q}b_q^{\dagger}\Big[\sum_{i,k}d_{qi}\mathcal{U}_{ikkq}\alpha_i\alpha_i^{\dagger}\alpha_k^{\dagger}\alpha_k\Big]b_q|\Psi_{\rm I}\rangle$$
$$-\Delta_{\rm nH}\langle\Psi_{\rm I}|\sum_{q}b_q^{\dagger}\Big[\sum_{i}d_{qi}d_{qi}^{*}\alpha_i\alpha_i^{\dagger}\Big]b_q|\Psi_{\rm I}\rangle\,, \tag{A19}$$

$$\langle\Psi_{\rm I}|[T_-,H_{\rm C}^{0}][H_{\rm C}^{0},T_+]|\Psi_{\rm I}\rangle$$
$$\approx\langle\Psi_{\rm I}|\sum_{q}b_q^{\dagger}\Big[\sum_{i,n,k}\mathcal{U}^{*}_{inq}\mathcal{U}_{jkkq}\alpha_n^{\dagger}\alpha_n\alpha_i\alpha_i^{\dagger}\alpha_k^{\dagger}\alpha_k\Big]b_q|\Psi_{\rm I}\rangle$$
$$+\tfrac{1}{2}\langle\Psi_{\rm I}|\sum_{q}b_q^{\dagger}\Big[\sum_{\substack{j,k\\ l(\neq j,k)}}\mathcal{U}^{*}_{jklq}\mathcal{U}_{jklq}\alpha_l^{\dagger}\alpha_k\alpha_j\alpha_j^{\dagger}\alpha_k^{\dagger}\alpha_l\Big]b_q|\Psi_{\rm I}\rangle\,. \tag{A20}$$

In order to understand our treatment of the Pauli principle, we consider the origins of the operators $\alpha^{\dagger}$ and α. The operator $\alpha_i\alpha_i^{\dagger}$ in Eqs. (A18) $\sim$ (A20)

owes its origin to the new-born proton. The operator $\alpha_k\alpha_j\alpha_j^\dagger\alpha_k^\dagger$ in Eq. (A20) is due partly to the new-born proton to which we assign the j-th state and partly to the recoil of its partner into the k-th state. On the other hand, the origins of the operators $\alpha_k^\dagger\alpha_k$ in Eq. (A19) and $\alpha_n^\dagger\alpha_n\alpha_k^\dagger\alpha_k$ and $\alpha_l^\dagger\alpha_l$ in Eq. (A20) are ascribed to the stationary source of the Coulomb forces which act on the new-born proton. If the Pauli principle is neglected for the new-born proton as $\alpha_i\alpha_i^\dagger\to 1$ and $\alpha_k\alpha_j\alpha_j^\dagger\alpha_k^\dagger\to\alpha_k\alpha_k^\dagger$ in Eqs. (A18)$\sim$(A20), they become

$$\langle\Psi_{\rm I}|T_-T_+|\Psi_{\rm I}\rangle\longrightarrow\langle\Psi_{\rm I}|\sum_q b_q^\dagger b_q|\Psi_{\rm I}\rangle\,, \tag{A21}$$

$$\langle\Psi_{\rm I}|T_-[H_{\rm C},\,T_+]|\Psi_{\rm I}\rangle\longrightarrow\langle\Psi_{\rm I}|\sum_q b_q^\dagger[\sum_k \mathcal{W}_{qkkq}\alpha_k^\dagger\alpha_k-\Delta_{\rm nH}]b_q|\Psi_{\rm I}\rangle\,, \tag{A22}$$

$$\begin{aligned}\langle\Psi_{\rm I}|[T_-,\,H_{\rm C}^0][H_{\rm C}^0,\,T_+]|\Psi_{\rm I}\rangle&\\ \longrightarrow\langle\Psi_{\rm I}|\sum_q b_q^\dagger[\sum_{j,n,k}\mathcal{W}_{jnnq}^*\mathcal{W}_{jkkq}\alpha_n^\dagger\alpha_n\alpha_k^\dagger\alpha_k]b_q|\Psi_{\rm I}\rangle&\\ +\tfrac{1}{2}\langle\Psi_{\rm I}|\sum_q b_q^\dagger[\sum_{\substack{j,k\\ l(\neq j,k)}}\mathcal{W}_{jklq}^*\mathcal{W}_{jklq}\alpha_l^\dagger\alpha_k\alpha_k^\dagger\alpha_l]b_q|\Psi_{\rm I}\rangle\,,&\end{aligned} \tag{A23}$$

where

$$\mathcal{W}_{jklq}=\sum_i d_{ji}\mathcal{U}_{iklq}\,, \tag{A24}$$

and use is made of Eq. (A9). This last step of our prescription corresponds to the neglect of the Pauli principle in the integrand of Eq. (17).

The right side of (A21) equals to the total number of neutrons N as is expected from the neglect of the Pauli principle. This is consistent with the equation

$$\int_{-\infty}^{\infty}dE\int_{\varepsilon_{\rm min}}^{\varepsilon_1}D_{\rm F}(E,\,\varepsilon)\frac{dN_1}{d\varepsilon}d\varepsilon=N_1=N\,, \tag{A25}$$

which is obtained from Eqs. (14) and (16). Actually, however, the lower limit of the integration domain over ε in our model (17) is $\varepsilon_0(E)$ which is not necessarily equal to $\varepsilon_{\rm min}$ as used in Eq. (A25). This modification of integration domain corresponds to the replacement of the operator of the new-born proton $\alpha_i\alpha_i^\dagger$ in Eq. (A18) by unity for unoccupied state and zero for occupied state, or more generally, by a weight function which lies between 0 and 1.

The two important properties of $D_{\rm F}(E,\,\varepsilon)$ as a function of E, namely, the center of the distribution and the second energy moment, can be inferred from the quantities in the square brackets of the right sides of (A22) and (A23). The meaning of these quantities can be seen directly or by transforming them into the coordinate representation. For simplicity, we neglect the exchange parts in the following arguments. The quantity in (A22) consists of the expectation value of the Coulomb energy that the new-born proton perceives in the average field and the neutron-hydrogen mass difference $\Delta_{\rm nH}$. The direct part of the first

quantity in (A23), $\sum_{j,n,k}\mathcal{W}^*_{jnnq}\mathcal{W}_{jkkq}\alpha_n^\dagger\alpha_n\alpha_k^\dagger\alpha_k$, equals to the expectation value of the square of the Coulomb energy that the new-born proton perceives in the average field if a minor change $\langle\alpha_n^\dagger\alpha_n\alpha_n^\dagger\alpha_n\rangle\to\langle\alpha_n^\dagger\alpha_n\rangle\langle\alpha_n^\dagger\alpha_n\rangle$ is made. In fact, the quantity can be written in the coordinate representation as

$$\int|\phi_q(\boldsymbol{r}_1)|^2\left[\int\rho(\boldsymbol{r}_2)\frac{e^2}{r_{12}}d\boldsymbol{r}_2\right]^2 d\boldsymbol{r}_1\,, \tag{A26}$$

where $\boldsymbol{r}_1$ designates the position of the new-born proton, and $\rho(\boldsymbol{r}_2)$ is the number density of proton in the parent nuclear state. In order to see the meaning of the second quantity in (A23), $\frac{1}{2}\sum_{j,k,l(\neq j,k)}\mathcal{W}^*_{jklq}\mathcal{W}_{jklq}\alpha_l^\dagger\alpha_k\alpha_k^\dagger\alpha_l$, we further replace $\alpha_k\alpha_k^\dagger$ by unity. Then, its direct part can be written as

$$\int|\phi_q(\boldsymbol{r}_1)|^2\left[\int\rho(\boldsymbol{r}_2)\left(\frac{e^2}{r_{12}}\right)^2 d\boldsymbol{r}_2\right]d\boldsymbol{r}_1 \tag{A27}$$

in the coordinate space provided that a minor change $\sum_{l(\neq j,k)}\to\sum_l$ is made. This is the expectation value of the sum of the squares of the Coulomb energies that the new-born proton feels from other individual protons which are allowed to recoil freely. Actually, the recoil is restricted by the presence of $\alpha_k\alpha_k^\dagger$, and the long-range part of the Coulomb interaction will be effectively attenuated, while the short-range part will be relatively unaffected. This latter part of the energy spread of $D_F(E,\varepsilon)$ seems to be relatively unimportant for medium and heavy nuclei, and has been neglected in our calculation in §§ 4 and 5.

An examination similar to the above-mentioned one will be possible also in the case of the Gamow-Teller transition if some suitable form of the nuclear potential is assumed. In this case, the latter part of the energy spread (A23) will play a more essential role because of the short-range nature of nuclear forces in contrast with the Fermi transition.

From the above formalism, the nature of the distribution function $D_2(E,\varepsilon)$ can be derived as has been stated at the end of § 3.

Appendix B

Approximate formulas for the f-function

In the analysis with the electronic computer we have used the following approximate formulas for the f-function or the integrated Fermi function.[26),27)] These formulas are correct to $\approx 10\%$ for usual β-decays. Although these approximations are rough, they seem to be sufficient for calculations such as ours. The units $\hbar=c=m_e=1$ are used, Z is the proton number of the daughter nucleus, and $E_0=-E$.

(1) For β^--decay:

$$f_-(Z,E_0)\approx a(Z)\cdot E_0^3+\frac{1}{g(Z,E_0)}E_0^4+c(Z)\cdot E_0^5+d(Z,E_0)\qquad\text{for } E_0\gtrsim 0\,,$$

where

$$a(Z)=1.52\cdot10^{-2}Z+6.40\cdot10^{-6}Z^3+8.50\cdot10^{-11}Z^5+1.70\cdot10^{-13}Z^7+2.50\cdot10^{-26}Z^{13},$$

$$c(Z)=3.33\cdot10^{-2}\exp(3.11\cdot10^{-2}Z),$$

$$d(Z,E_0)=0.132E_0^{7/2}\exp(-0.5Z)/(1+2.805E_0^5),$$

$$g(Z,E_0)=b_1(Z)+\left(\frac{E_0-b_3(Z)}{b_2(Z)}\right)^5,$$

with

$$b_1(Z)=5.26\exp(-6.65674\cdot10^{-3}Z-6.41863\cdot10^{-5}Z^2-7.00193\cdot10^{-6}Z^3+4.74649\cdot10^{-8}Z^4),$$

$$b_2(Z)=9.80-7.03\cdot10^{-2}Z-1.28\cdot10^{-3}Z^2+2.84\cdot10^{-5}Z^3,$$

$$b_3(Z)=2.0\exp(-0.5Z)+8.5+6.0\cdot10^{-4}Z^2.$$

(2) For β^+-decay and electron capture:

$$f_+(Z,E_0)=f_++f_\epsilon=f_K[(f_+/f_K)+1+(f_L/f_K)+\cdots],$$

where

$$f_K=\frac{\pi}{2}g_K^2(E_0-1+W_K)^2 \quad \text{for } E_0\geqq1-W_K,$$

with

$$g_K^2=4(1+s)(\alpha Z_0)^{2s+1}(2R)^{2s-2}\exp(-2\alpha Z_0R)/\Gamma(2s+1),$$

$$R=\tfrac{1}{2}\alpha A^{1/3} \quad (\alpha \text{ is the fine structure constant}),$$

$$W_K=\sqrt{1-(\alpha Z_0)^2}=s,$$

$$\Gamma(2s+1)\approx\sqrt{2\pi}(2s)^{2s+1/2}\exp(-2s)\left\{1+\frac{1}{12}\left(\frac{1}{2s}\right)+\frac{1}{288}\left(\frac{1}{2s}\right)^2-\frac{139}{51840}\left(\frac{1}{2s}\right)^3-\frac{571}{2488320}\left(\frac{1}{2s}\right)^4+\cdots\right\} \text{(Stirling)},$$

$$Z_0=Z+1,$$

$$f_+/f_K\approx\frac{(E_0-2)^4}{a(Z)+b(Z)(E_0-2)} \quad \text{for } E_0\geqq2,$$

with

$$a(Z)=10^{1.56Z^{0.363}-4.60},$$

$$b(Z)=5.4926\cdot10^{-3}\exp\{-0.2375\log Z+3.179(\log Z)^2\},$$

and

$$f_L/f_K\approx(f_{L_I}/f_K)(1+(f_{L_{II}}/f_{L_I})),$$

with

$$f_{L_I}/f_K = \frac{g_{L_I}^2}{g_K^2}\left(\frac{E_0-1+W_{L_I}}{E_0-1+W_K}\right)^2 \quad \text{for } E_0 \geqq 1-W_L$$

$$\approx (6.89\cdot 10^{-2}+6.77\cdot 10^{-4}Z_0+2.58\cdot 10^{-6}Z_0^2+2.20\cdot 10^{-8}Z_0^3) \times \left(\frac{E_0-1+W_{L_I}}{E_0-1+W_K}\right)^2,$$

$$f_{L_{II}}/f_{L_I} = \frac{f_{L_{II}}^2}{g_{L_I}^2} = \frac{W_L-s}{W_L+s}\left[1+\frac{2\alpha Z_0 R}{(s+1)(2s+1)-\alpha Z_0 R(2W_L+1)}\right]^2,$$

$$W_{L_I} = W_{L_{II}} = W_L = \sqrt{(1+s)/2}\,.$$

The L_{III}, M, N and O captures are neglected.

References

1) e. g. E. J. Konopinski, *The Theory of Beta Radioactivity* (Oxford Univ.Press, New York, 1966), Chap. 5.
2) J. Żylicz, P. G. Hansen, H. L. Nielsen and K. Wilsky, Ark. Fysik **36** (1967), 643.
3) A. Arima and H. Horie, *Proceedings of the Rehovoth Conference on Nuclear Structure* (1957), p. 215.
   C. A. Caine, Proc. Phys. Soc. **A71** (1958), 939.
4) I. Hamamoto, Nucl. Phys. **62** (1965), 49; **66** (1965), 176.
   A. B. Migdal, Nucl. Phys. **57** (1957), 29; *Theory of Finite Fermi Systems and Applications to Atomic Nuclei* (Interscience Publishers, New York, 1967) [*Teoriya Konechnykh Fermi-Sistem i Svoĭstva Atomnykh Yader* (Pub. "Nauka", Moscow, 1965)].
5) J. D. Anderson, C. Wong and J. W. MacClure, Phys. Rev. **126** (1962), 2170; **129** (1963), 2718.
6) J. D. Fox and D. Robson (editor), *Isobaric Spin in Nuclear Physics* (Academic Press, New York - London, 1966).
7) A. M. Lane and J. M. Soper, Nucl. Phys. **37** (1962), 663.
8) R. P. Feynman and M. Gell-Mann, Phys. Rev. **109** (1958), 193.
   S. S. Gershtein and Ya. B. Zel'dovich, Zh. Eksp. i Teor. Fiz. **29** (1955), 698[Soviet Phys.-JETP **2** (1957), 576].
9) W. P. Alford and J. B. French, Phys. Rev. Letters **6** (1961), 119.
   S. D. Bloom, in reference 6), p. 123.
10) K. Ikeda, S. Fujii and J. I. Fujita, Phys. Letters **3** (1963), 271.
    J. I. Fujita, S. Fujii and K. Ikeda, Phys. Rev. **133** (1964), B549.
    K. Ikeda, Prog. Theor. Phys. **31** (1964), 434.
    J. I. Fujita and K. Ikeda, Nucl. Phys. **67** (1965), 145.
11) J. I. Fujita, Y. Futami and K. Ikeda, Prog. Theor. Phys. **38** (1967), 107.
12) J. I. Fujita, Y. Futami and K. Ikeda, *Proceedings of the International Conference on Nuclear Structure, Tokyo, 1967* (Suppl. J. Phys. Soc. Japan **24** (1968)), p. 437.
13) J. I. Fujita and K. Ikeda, Prog. Theor. Phys. **36** (1966), 288.
14) M. Yamada, Soryushiron Kenkyu (mimeographed circular in Japanese) **26** (1963), 534; Bull. Sci. Eng. Res. Lab., Waseda Univ. No. 31/32 (1965), 146.
15) e. g. K. Siegbahn (editor), *Alpha-, Beta- and Gamma-Ray Spectroscopy* (North-Holland Publishing Co., Amsterdam, 1965), Chap. XXIII.
16) E. M. Henley, in reference 6), p. 3.
17) K. A. Brueckner and J. L. Gammel, Phys. Rev. **109** (1958), 1023.
18) F. J. Dyson, J. Math. Phys. **3** (1962), 140.

19) K. Way et al., *Nuclear Data Sheets* (National Academy of Sciences, National Research Council, Washington, D. C., 1958–65); *Nuclear Data* **B-1** (Academic Press, New York-London, 1966).
20) M. Yamada and Z. Matumoto, J. Phys. Soc. Japan **16** (1961), 1497.
21) J. Bardeen, L. N. Cooper and J. R. Schriffer, Phys. Rev. **108** (1957), 1175.
22) S. T. Belyaev, Kgl. Danske Viedenskab. Selskab, Mat.-fys. Medd. **31** (1959), No. 11.
L. S. Kislinger and R. A. Sorensen, Kgl. Danske Viedenskab. Selskab, Mat.-fys. Medd. **32** (1960), No. 9.
23) A. H. Wapstra, *Handbuch der Physik* (Springer-Verlag, Berlin, 1958), Vol. XXXVIII/1, p. 1.
24) H. Ejiri, J. Phys. Soc. Japan **22** (1967), 360.
25) Z. Matumoto and M. Yamada, Prog. Theor. Phys. **19** (1958), 285.
L. Van Neste, R. Coussement and J. P. Deutsch, Nucl. Phys. **98** (1967), A585; **102** (1967), A369.
26) E. Feenberg and G. Trigg, Rev. Mod. Phys. **22** (1950), 399.
27) M. E. Rose, *Relativistic Electron Theory* (John Wiley & Sons Inc., New York, 1960), Chap. V.
H. Brysk and M. E. Rose, Rev. Mod. Phys. **30** (1958), 1169.